

# Elastic Properties and Short-to Medium-Range Order in Glasses

Tanguy Rouxel<sup>†</sup>

LARMAUR, FRE CNRS 2717, Université de Rennes 1, Campus de Beaulieu, 35042 Rennes cedex, France

Very different materials are named “Glass,” with Young’s modulus ( $E$ ) and Poisson’s ratio ( $\nu$ ) extending from 5 to 180 GPa and from 0.1 to 0.4, respectively, in the case of bulk inorganic glasses. Although glasses have in common the lack of long-range order in the atomic organization, they offer a wide range of structural features at the nanoscale and we show in this analysis that beside the essential role of elastic properties for materials selection in mechanical design, the elastic characteristics ( $E$ ,  $\nu$ ) at the continuum scale allow to get insight into the short- and medium-range orders existing in glasses. In particular,  $\nu$ , the atomic packing density ( $C_g$ ) and the glass network dimensionality appear to be strongly correlated. Maximum values for  $\nu$  and  $C_g$  are observed for metallic glasses ( $\nu \sim 0.4$  and  $C_g > 0.7$ ), which are based on cluster-like structural units. Atomic networks consisting primarily of chains and layers units (chalcogenides, low Si-content silicate, and phosphate glasses) correspond to  $\nu > 0.25$  and  $C_g > 0.56$ . On the contrary,  $\nu < 0.25$  is associated with a highly cross-linked network, such as in  $\alpha$ -SiO<sub>2</sub>, with a tri-dimensional organization resulting in a low packing density. Moreover, the temperature dependence of the elastic moduli brings a new light on the structural changes occurring above the glass transition temperature and on the depolymerization rate in the supercooled liquid. The softening rate depends on the level of cooperativity of atomic movements at the source of the deformation process, with an obvious correlation with the “fragility” of the liquid.

## I. Introduction

ELASTIC properties are intimately related to the fine details of the atomic packing characteristics. Because there is a large diversity of glasses, with different atomic bond types and a great variety of atomic organization, elastic moduli cover a large range of values. *On the one hand*, recalling that elastic moduli are expressed in Pascals, i.e., in J/m<sup>3</sup>, the magnitude of the elastic moduli is governed by both the atomic bond energy (subnanometer scale) and the atomic packing density ( $C_g$ ). *On the other hand* there seems to be a direct correlation between  $\nu$  and the degree of symmetry of the structural units existing at the

D. Green—contributing editor

Manuscript No. 23132. Received April 25, 2007; approved June 21, 2007.

<sup>†</sup>Author to whom correspondence should be addressed. e-mail: tanguy.rouxel@univ-rennes1.fr

molecular scale (nanometer size). Correlatively, the temperature dependence of  $\nu$  above  $T_g$  gives some insight into the magnitude of the depolymerization process occurring in the liquid. The elastic properties of glasses from very different chemical systems were compared and interpreted in the light of their ( $C_g, \nu$ ) values and of the recent literature on the thermodynamics and the structure of glass networks. Poisson’s ratio, which covers a wide interval of values for inorganic glasses, thus plays a peculiarly interesting role and deserves a special focus in this article devoted to the relationship between elasticity and the atomic structure of glasses. Besides, the temperature dependence of the elastic moduli provides a new insight into the glass transition phenomenon and is very sensitive to the glass composition. The softening rate observed above the glass transition temperature ( $T_g$ ), i.e., in the supercooled liquid range, can be discussed in the light of the heterogeneity of the nature of the interatomic bonding and is correlated with the liquid fragility.

The chemical design of glasses with high elastic moduli is another important issue in glass science and some basic guidelines can be drawn from the present analysis. Although this is a rather old topic, there is still much to do in this area, and contrary to the common belief, there are low  $T_g$  glasses with relatively high elastic moduli and vice versa.

Therefore, the elastic properties of glasses, which are readily experimentally available parameters (it takes  $\sim 15$  min to measure the transverse and longitudinal wave velocities and further to calculate  $E$  and  $\nu$  by means of ultrasonic echography (USE) using piezoelectric transducers<sup>1</sup> (Panel A)), allow to probe the short- to medium-range order in glasses, as well as the structural changes occurring upon temperature or pressure changes, which are of paramount interest for glass scientists. The aim of this article is not to provide an exhaustive review of the glass elastic properties reported so far but to put some light on the intimate relationships existing between the elastic moduli and the fine detail of the atomic network organization.

## II. Overview of the Elastic Properties of Glasses

### (1) Different Glass Systems

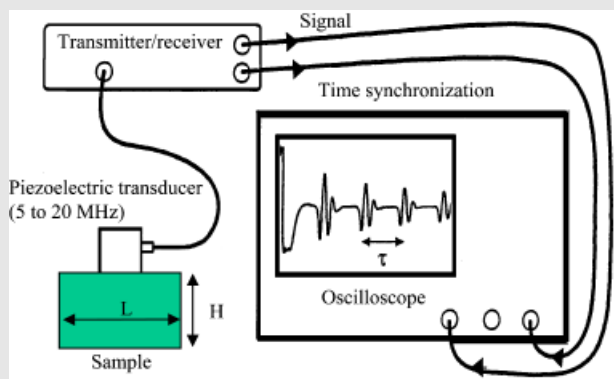
This review is focused on inorganic glasses, including soft and brittle chalcogenide<sup>2–16</sup> glasses on one side and high-performance bulk metallic,<sup>17–22</sup> rare-earth,<sup>23–31</sup> silicon oxynitride,<sup>32–53</sup> and oxycarbide<sup>54–59</sup> glasses on the other side (Fig. 1, Table I), not omitting the widely used alkali–alkaline-earth–silicate and aluminosilicate or boro-silicate glasses,<sup>61,70,73–75,77,80–88</sup> borate,<sup>71,72,89–91</sup> phosphate,<sup>62–65,92–99</sup> germanate,<sup>67–69,100–102</sup> and the naturally occurring basaltic glasses.<sup>76,103</sup>

# Feature

### Panel A: Ultrasonic Echography Methods (USE)

#### Measurement of elastic moduli by ultrasonic echography

##### Measurement at ambient temperature



Elastic wave in semi-infinite medium:  $\lambda \ll L$  and  $\lambda \ll H$

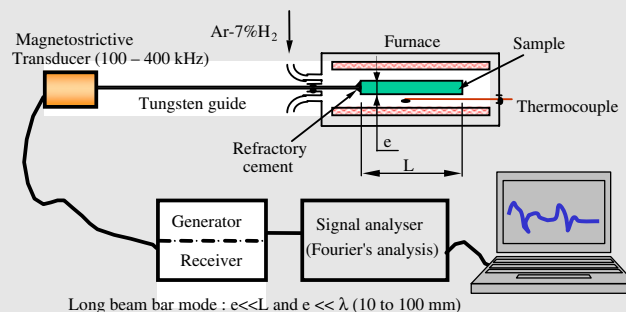
$$E = \rho(3V_l^2 - 4V_t^2)/(V_l/V_t)^2 - 1)$$

$$G = \rho V_t^2$$

$$\nu = E/(2G) - 1$$

Where  $\rho$  is the specific mass,  $V_l$  the longitudinal wave velocity,  $V_t$  the transverse wave velocity.

##### High temperature measurements



Long beam bar mode:  $e \ll L$  and  $e \ll \lambda$  (10–100 nm)

$$E = \rho V_l^2$$

##### Small size specimens: acoustic microscopy

When  $(L, H) < \lambda$ , regular piezoelectric transducers are unable to efficiently promote the propagation of shear waves through the specimen. Focused piezoelectric transducers can be used to propagate surface-type waves, also called Rayleigh waves, which velocity is given by:  $V_R = \zeta V_t$ , where  $\zeta$  is a function of Poisson's ratio, or of the  $V_l/V_t$  ratio.  $V_R$  and  $V_l$  are measured and  $V_t$  is optimized to satisfy the following equation:

$$V_R = \frac{V_l(0.715 - (V_t/V_l)^2)}{0.750 - (V_t/V_l)^2}$$

(A) *Amorphous Ice*<sup>60,104–108</sup>. Even though ice is a mineral, there exist also different amorphous phases for solid water. Amorphous ice<sup>60,107</sup> consists of water molecules that are randomly orientated, and can be synthesized by ultra-fast cooling of liquid water (cooling rate typically of the order of  $10^6$  K/s) below 120 K. Note that glassy ice is the dominant state of solid water in the universe (comets are mainly composed of glassy ice). Despite relatively strong intramolecular H–O bonds (bonding energy  $\sim 492$  kJ/mol), close to the Al–O bond strength for instance, the intermolecular bonding between hydrogen and a neighboring oxygen atom of another water molecule (hydrogen bonding) has an optimal energy of 23 kJ/mol, and being the weakest link of the atomic network, it governs the stiffness. Consequently,  $E$  ranges between 8 for the low-density phase ( $\rho = 0.93$  g/cm<sup>3</sup>) and 11 GPa for the densest one ( $\rho = 1.17$  g/cm<sup>3</sup>).<sup>104,106,108</sup>

(B) *Chalcogenide Glasses*: Chalcogenide glasses<sup>2,9,12</sup> combine elements from the 16th column (VIB group) of Mendeleiev periodic table with metallic and/or semiconductor ones from the 13th to 15th columns. They are based on strong intramolecular covalent bonds between chain-forming chalcogen atoms (S, Se, and Te) and with atoms of higher coordination (As(3), Sb(3), and Ge(4)) forming interchain bridges, and weak van der Waals bonds between chains and/or layers. As a consequence of this weak intermolecular bonding, in spite of high covalent bond energies (200–400 kJ/mol), close to those of the Si–N and Si–C bonds, relatively soft and compliant glasses are obtained:  $E < 25$  GPa ( $T_g < 620$  K). Unfortunately, heavy chalcogenide (or halide) elements that lower the phonon vibration energy and thus enhance the infrared (IR) transparency are weakly coordinated elements (mostly twofold) and are thus detrimental to the network cross linking and to the mechanical properties. Compared with traditional germanium-based IR optics, they are cheaper and can be more easily shaped into optical parts. Applications are mostly based on the transparency in the second atmospheric window (6 to 15 microns) and include optical components such as IR lenses, fibers, windows, and filters for thermal imaging systems.

(C) *Halide Glasses*: Halide glasses<sup>7,9,10,16</sup> combine metals with F, Cl, Br, and I (group VII of the periodic chart). The weakness of the halide-metal bond results in low  $T_g$  temperatures, typically lower than 673 K, and a poor chemical durability (usually stronger bonds form between the metal and O, OH, or H<sub>2</sub>O). Consequently, only a few halide glasses may find practical applications among which the heavy-metal ZBLAN grades (fluorine combined with Zr, Ba, La, Al, Na, hence the name) are being increasingly used for passive IR optics and for the containment of corrosive fluorine compounds. In comparison with a-SiO<sub>2</sub> that is transparent for wavelengths from 0.3 to 4  $\mu$ m, fluoride glasses are transparent from 0.2 to over 9  $\mu$ m. Their  $E$  and  $T_g$  values are typically  $\sim 50$ –60 GPa and  $\sim 535$ –545 K, respectively. They are also good candidates for active IR optics and long-distance telecommunications.

(D) *Borates*: Although boron is one of the best-known glass formers and forms strong atomic bonding with oxygen ( $U_{O-B-O} \sim 809$  kJ/mol), amorphous boron oxide (a-B<sub>2</sub>O<sub>3</sub>) and borate-rich glasses have relatively low elastic moduli ( $\sim 17$  GPa for pure a-B<sub>2</sub>O<sub>3</sub>)<sup>66,70</sup> and  $T_g$  because the atomic network is built on corner-sharing BO<sub>3</sub> planar triangles, which are weakly bonded together—unlike crystallized B<sub>2</sub>O<sub>3</sub> consisting of a tri-dimensional cross-linked network (trigonal symmetry). Some medium-range order shows up in a-B<sub>2</sub>O<sub>3</sub> with the occurrence of boroxol rings composed of three corner-sharing BO<sub>3</sub> triangles forming an equilateral triangle.<sup>90</sup> The addition of cations such as Na, Li, or Pb favors boron in tetrahedral coordination and enhances the elastic moduli<sup>70,71</sup> as well as  $T_g$ .

(E) *Phosphate Glasses*: Phosphate glasses<sup>62,64,92</sup> possess remarkable functional properties such as low dispersion and high refractive indices, high transparency in the ultraviolet range (alkaline-earth phosphate glasses), and large rare-earth-stimulated emission cross sections combined with low thermo-optical coefficients, which make them excellent candidates for power laser applications (Nd-doped aluminophosphate glasses are the most widely used glasses for laser).<sup>64,98</sup> Alkali aluminophosphate glasses have a relatively large thermal expansion coefficient and are suitable for glass–metal welding or seal-

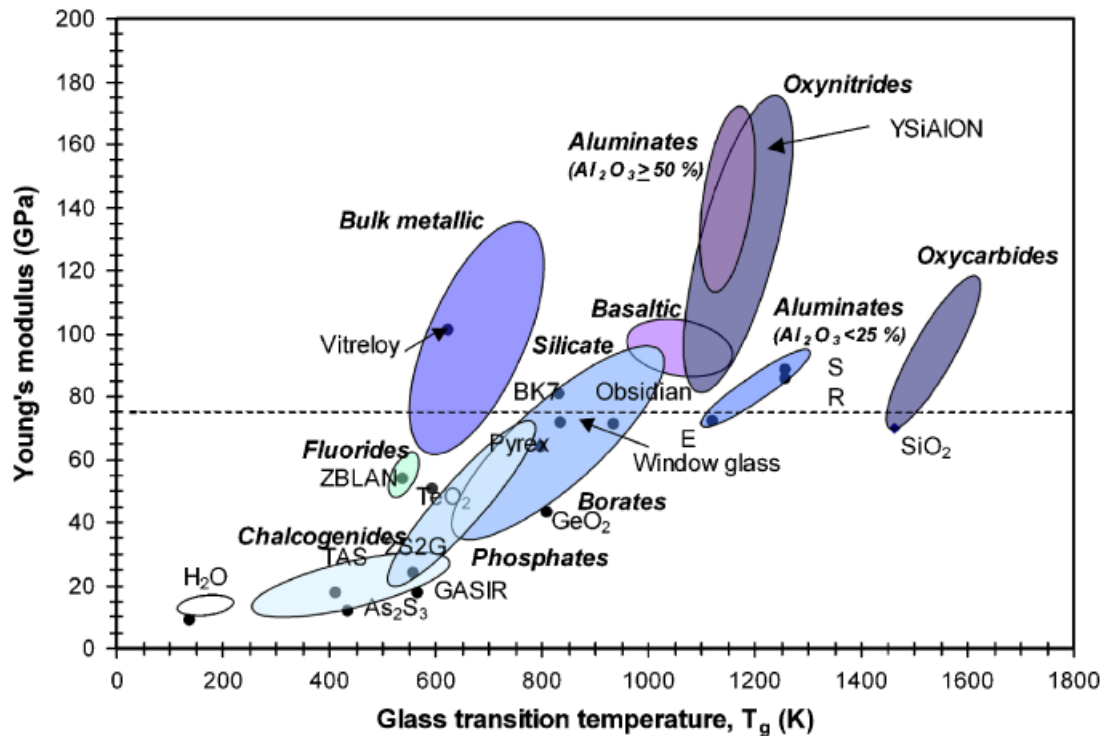


**Fig. 1.** Young's modulus at 293 K (except for amorphous ice for which data were obtained at 77 K) and glass transition temperatures for different inorganic glass chemical systems. Some commercially available glasses are also plotted with their standard denomination: TAS, 2S2G (Schott Glass Co.), and GASIR (Umicore Infrared Co.) stand for  $\text{Te}_2\text{As}_3\text{Se}_5$ ,  $\text{Ga}_2\text{Ge}_{20}\text{Sb}_{10}\text{S}_{65}$ , and  $\text{Ge}_{22}\text{As}_{20}\text{Se}_{58}$ , respectively. ZBLAN (Le Verre Fluoré Ltd.) is a heavy metal fluoride glass with typical composition  $\text{F}_{0.753}\text{Zr}_{0.141}\text{Ba}_{0.041}\text{La}_{0.008}\text{Al}_{0.012}\text{Na}_{0.045}$ . *E*, *R*, and *S* glasses are high-strength industrial aluminosilicate glasses with 16 (*E*) to 25 (*S*) mol%  $\text{Al}_2\text{O}_3$ . Pyrex (Corning) and BK7 (Schott) are borosilicate glasses synthesized with about 12 and 10 mol% boric oxide. BK7 is a crown glass (alkali-lime silicate containing approximately 10% potassium oxide) used in precision lenses whereas Pyrex is mostly used for its thermal shock resistance and its chemical durability. Obsidian and basaltic glasses are naturally occurring materials. Vitreloy is the name of a Zr-based bulk metallic glass with composition  $\text{Zr}_{41}\text{Ti}_{14}\text{Cu}_{12.5}\text{Ni}_{10}\text{Be}_{22.5}$  (Liquidmetal Tech. Ltd., CA), which behaves purely elastic up to 1.5 GPa. YSiAlON(s) are silicon oxynitride glasses synthesized from  $\text{Si}_3\text{N}_4$ ,  $\text{SiO}_2$ ,  $\text{Al}_2\text{O}_3$ , AlN, and  $\text{Y}_2\text{O}_3$  with up to 15 at.% nitrogen. Silicon oxynitride glasses exhibit  $T_g$  above 1123 K, Young's moduli > 150 GPa, and are observed at grain boundaries in liquid-phase-sintered silicon nitride ceramics. Silicon oxycarbide glasses are polymer- or gel-derived glasses, which have the highest  $T_g$  ever reported for glasses so far to the best of the knowledge of the author.

ing applications (in particular with aluminum).<sup>99</sup> Some typical laser glasses have Young's moduli between 45 and 50 GPa and  $T_g$  between 640 and 760 K.<sup>64</sup> Iron phosphates possess Young's moduli as high as the one of a-SiO<sub>2</sub>.<sup>63</sup> Phosphate glasses are also presently considered for use in optical fibers for laser surgery. Glasses from the  $\text{Na}_2\text{O}$ -CaO-SiO<sub>2</sub>-P<sub>2</sub>O<sub>5</sub> system with about 5–7 mol% P<sub>2</sub>O<sub>5</sub> are biocompatible and are very attractive materials for the fabrication of prosthesis or implant (eventually with therapeutic substances) allowing for a perfect bonding to the human bones.<sup>65,93</sup> In this latter case, elastic properties are of paramount importance to adapt the mechanical properties of the implant to one of the body parts in contact. These bioglasses have  $T_g$  from 725 to 803 K and *E* between 35 and 90 GPa. The major weakness of phosphate glasses lies in their poor chemical durability and especially their sensitivity to water. Addition of  $\text{Al}_2\text{O}_3$  or  $\text{B}_2\text{O}_3$  enhances the durability but a more significant improvement is obtained by adding nitride compounds to the melt or by treating the melt in anhydrous ammonia gas. In this latter case, nitrogen increases the cross-linking density and the P–N bonds, more covalent than the P–O ones, enhance the chemical durability.<sup>94,96</sup> Phosphorous oxynitride glasses are composed of  $\text{PO}_4$ ,  $\text{PO}_3\text{N}$ , and  $\text{PO}_2\text{N}_2$  tetrahedra. Note that PON glass is a silica analog in which  $\text{PO}_2\text{N}_2$  tetrahedra share their four corners. See the review by Brow<sup>97</sup> for further details on the structure of phosphate glasses.

(*F*) **Germanate Glasses:**  $\text{GeO}_2$ -based glasses<sup>67,100,101</sup> are transparent in the 2–6  $\mu\text{m}$  IR wavelength range and possess a good chemical durability. The thermal properties of germanates are comparable with those of silicates, which have smaller cations and anions and thus have a lower IR cutoff.<sup>67,69</sup> In addition, germanate glasses possess relatively low absorption loss and suitable thermo-optic coefficient for high-energy laser

(HEL) applications,<sup>68</sup> and in comparison with zinc sulfide (ZnS), which is typically used as an exit window for HEL applications, barium gallo-germanate (BGG) glasses are ~3 times harder, are isotropic, and have excellent transmission in visible and mid-IR region.

(*G*) **Silicate and Aluminate Glasses:** Silicate glasses usually contain up to 60–70 mol% SiO<sub>2</sub>. Usual additives include alkaline and alkaline-earth oxides among which Na<sub>2</sub>O and CaO are the most common in window glass compositions. In oxide glasses, when the bonding energy between a cation and an oxygen atom is > 500 kJ/mol, this cation is considered as a network former.<sup>109</sup> Such elements (P, Al, Ge, Zr, Si, and B) gave their names to different oxide glass families with  $T_g$  ranging between 600 and 1300 K and Young's modulus between 30 and 100 GPa, the highest values being attributed to the alumina-rich compositions.<sup>24–26,28,81,82</sup> *E* and *R* glasses are aluminosilicate glasses with about 15 and 24 mol%  $\text{Al}_2\text{O}_3$ .<sup>110</sup> *E* glass also contains boron, calcium, and magnesium and was developed originally for use as an insulator in the electric industry. It turns out that its mechanical properties are pretty good too, so that it found large-scale industrial applications both in the textile industry and for reinforcement in polymer matrix composites. *R* (or *S*) glass was designed to meet high strength and stiffness for reinforcement (in the form of fibers). Rare-earth aluminosilicates with more than 50 mol%  $\text{Al}_2\text{O}_3$  reach *E* values as high as 169 GPa but can hardly be prepared as bulk microcrystal-free materials. Naturally occurring glasses include basaltic glasses,<sup>76,103</sup> which are Al- or Mg-rich silicates with 45–65 mol% SiO<sub>2</sub>, by far the most abundant and used for the production of insulation fibers, obsidian, a glass produced by volcanoes when a felsic lava cools rapidly, which contain over 70 mol% SiO<sub>2</sub> and to a much lesser extent tectonic glasses resulting from the ex-

Table I. Some Elastic Moduli and  $T_g$  of Inorganic Glasses from Various Chemical Systems at 293 K

Chemical systems	Glass composition	$E$ (GPa)	$K$ (GPa)	$\nu$	$T_g$ (K)	References
Water	Glassy ice (H <sub>2</sub> O, high-density grade)	12.5 <sup>†</sup>	9.9 <sup>†</sup>	0.290 <sup>†</sup>	~136	[60]
Chalcohalogenides	Se	10.3	9.6	0.322	313	[11]
	Ge <sub>10</sub> Se <sub>90</sub>	12.1	10.4	0.307	365	[14]
	Ge <sub>15</sub> Se <sub>85</sub>	13.8	11.2	0.295	383	[14]
	Ge <sub>25</sub> Se <sub>75</sub>	16.1	12.3	0.281	501	[14]
	Ge <sub>30</sub> Se <sub>70</sub>	17.9	12.6	0.264	573	[14]
	As <sub>2</sub> S <sub>3</sub>	16.5	13.8	0.30	465	/
	Se <sub>83</sub> Te <sub>17</sub>	17.8	11.47	0.323	~350	[11]
	Ge <sub>22</sub> As <sub>20</sub> Se <sub>58</sub> (Umicore Infrared Co.)	18	13.6	0.28	565	/
	Ge <sub>18.2</sub> Sb <sub>18.2</sub> Se <sub>63.6</sub>	20.35	15.21	0.277	524	[11]
	Ge <sub>13.3</sub> Sb <sub>23.3</sub> Se <sub>63.4</sub>	21.69	15.65	0.269	512	[11]
	Ge <sub>23.3</sub> Sb <sub>3.3</sub> Se <sub>73.3</sub>	16.94	13.44	0.290	474	[11]
	Ge <sub>13.3</sub> Sb <sub>3.3</sub> Se <sub>83.5</sub>	14.25	11.76	0.298	386	[11]
	Ge <sub>30</sub> Sb <sub>10</sub> Se <sub>60</sub>	21.58	14.74	0.256	565	[11]
	Ge <sub>15</sub> Sb <sub>5</sub> Se <sub>80</sub>	15.0	12.1	0.293	411	[14]
	Ge <sub>15</sub> Sb <sub>10</sub> Se <sub>75</sub>	17.1	13.2	0.284	432	[14]
	Ge <sub>15</sub> Sb <sub>15</sub> Se <sub>70</sub>	19.2	14.3	0.276	457	[14]
	Ge <sub>15</sub> Sb <sub>20</sub> Se <sub>65</sub>	20.5	14.6	0.266	498	[14]
	Ge <sub>15</sub> Sb <sub>25</sub> Se <sub>60</sub>	22.6	15.9	0.263	507	[14]
	Te <sub>2</sub> As <sub>3</sub> Se <sub>5</sub> (TAS)	18	13.6	0.28	410	[14]
	Ga <sub>5</sub> Sb <sub>10</sub> Ge <sub>25</sub> Se <sub>60</sub> (2S2G, Schott)	23.9	16.7	0.262	556	[14]
F <sub>0.753</sub> Zr <sub>0.141</sub> Ba <sub>0.041</sub> La <sub>0.008</sub> Al <sub>0.012</sub> Na <sub>0.045</sub> (ZBLAN - Le Verre Fluoré Ltd.)	54.3	43.1	0.29	538	/	
Lead-containing	Si <sub>0.22</sub> Na <sub>0.024</sub> K <sub>0.076</sub> Ca <sub>0.005</sub> Pb <sub>0.09</sub> O <sub>0.585</sub> ("Cristal" type)	61	36.3	0.22	747	[12]
	V <sub>0.27</sub> Pb <sub>0.03</sub> O <sub>0.7</sub>	42	35.0	0.30	ND	[61]
	V <sub>0.25</sub> Pb <sub>0.06</sub> O <sub>0.69</sub>	48	44.4	0.32	ND	[61]
Phosphates	P <sub>2</sub> O <sub>5</sub>	31.3	24.8	0.29	650	[62]
	P <sub>2</sub> Na <sub>2</sub> O <sub>7</sub>	35.9	ND	ND	647	[62]
	P <sub>2</sub> CaO <sub>6</sub>	55.3	ND	ND	713	[62]
	LiPO <sub>3</sub>	46.3	35.1	0.28	ND	[62]
	Fe <sub>0.06</sub> P <sub>0.242</sub> O <sub>0.697</sub>	71.5	46.7	0.24	ND	[63]
	Fe <sub>0.077</sub> P <sub>0.231</sub> O <sub>0.693</sub>	70.4	45.8	0.24	ND	[63]
	Fe <sub>0.094</sub> P <sub>0.219</sub> O <sub>0.688</sub>	70.9	46.3	0.24	ND	[63]
	Fe <sub>0.111</sub> P <sub>0.206</sub> O <sub>0.683</sub>	73.2	48	0.25	ND	[63]
	Fe <sub>0.129</sub> P <sub>0.194</sub> O <sub>0.677</sub>	72.3	47.2	0.24	ND	[63]
Aluminophosphate <sup>‡</sup>	Hoya LHG-80	50	36.2	0.27	675	[64]
	Hoya LHG-8	50	34.7	0.26	758	[64]
	Schott LG-770	47	31.3	0.25	734	[64]
	Schott LG-750	50	34.7	0.26	723	[64]
	Kigre Q88	70	44.9	0.24	640	[64]
(Ca,Na)-Silicophosphate <sup>§</sup>	Si <sub>0.144</sub> Na <sub>0.171</sub> Ca <sub>0.086</sub> P <sub>0.04</sub> O <sub>0.559</sub>	83.5	58.8	0.263	782	[65]
	Si <sub>0.150</sub> Na <sub>0.164</sub> Ca <sub>0.082</sub> P <sub>0.04</sub> O <sub>0.564</sub>	84.2	62	0.274	803	[65]
	Si <sub>0.165</sub> Na <sub>0.146</sub> Ca <sub>0.073</sub> P <sub>0.04</sub> O <sub>0.576</sub>	81.3	58.9	0.270	757	[65]
	Si <sub>0.181</sub> Na <sub>0.128</sub> Ca <sub>0.064</sub> P <sub>0.039</sub> O <sub>0.588</sub>	76.6	57.8	0.279	725	[65]
Germanates	GeO <sub>2</sub>	43.3	23.28	0.19	808	[66]
	BaO-Ga <sub>2</sub> O <sub>3</sub> -GeO <sub>2</sub> type (BGG)	63.6	53	0.30	923	[67,68]
	Ge <sub>0.154</sub> Ga <sub>0.154</sub> La <sub>0.062</sub> O <sub>0.636</sub>	106.4	94.7	0.313	ND	[69]
	Ge <sub>0.148</sub> Ga <sub>0.148</sub> La <sub>0.074</sub> O <sub>0.636</sub>	104.1	94.8	0.317	ND	[69]
	Ge <sub>0.14</sub> Ga <sub>0.14</sub> La <sub>0.092</sub> O <sub>0.636</sub>	105	96.2	0.318	ND	[69]
	Ge <sub>0.125</sub> Ga <sub>0.125</sub> La <sub>0.125</sub> O <sub>0.636</sub>	103.8	97.7	0.323	ND	[69]
Borates and borosilicates	B <sub>2</sub> O <sub>3</sub>	17.4	12.1	0.26	541	[66]
	Na <sub>0.02</sub> B <sub>0.39</sub> O <sub>0.59</sub>	26	19	0.257	ND	[70]
	Na <sub>0.046</sub> B <sub>0.374</sub> O <sub>0.58</sub>	33	25	0.278	ND	[70]
	Na <sub>0.073</sub> B <sub>0.356</sub> O <sub>0.571</sub>	39	29	0.267	ND	[70]
	Na <sub>0.096</sub> B <sub>0.342</sub> O <sub>0.562</sub>	47	35	0.280	ND	[70]
	B <sub>0.316</sub> Pb <sub>0.105</sub> O <sub>0.579</sub>	61.7	40.0	0.243	ND	[71]
	B <sub>0.312</sub> Pb <sub>0.104</sub> O <sub>0.5580</sub> F <sub>0.026</sub>	62.6	40.6	0.243	ND	[71]
	B <sub>0.312</sub> Pb <sub>0.104</sub> O <sub>0.558</sub> F <sub>0.026</sub>	66.7	43.2	0.243	ND	[71]
	B <sub>0.308</sub> Pb <sub>0.103</sub> O <sub>0.538</sub> F <sub>0.0513</sub>	61.8	40.1	0.243	ND	[71]
	B <sub>0.304</sub> Pb <sub>0.101</sub> O <sub>0.519</sub> F <sub>0.076</sub>	71.3	46.3	0.243	ND	[71]
	B <sub>1.85</sub> CS <sub>0.15</sub> O <sub>2.925</sub>	24.8	19.45	0.288	ND	[72]
	Schott BK7	81	46.6	0.21	830	/
	Schott Borofloat	63	32.8	0.18	803	/

Table I. Continued

Chemical systems	Glass composition	<i>E</i> (GPa)	<i>K</i> (GPa)	$\nu$	<i>T<sub>g</sub></i> (K)	References	
	Si <sub>0.25</sub> Al <sub>0.011</sub> B <sub>0.072</sub> Na <sub>0.027</sub> O <sub>0.64</sub> (Corning Pyrex 7740)	64	35.6	0.2	798	/	
Alkali-alkaline-earth-silicates	SiO <sub>2</sub> (Vitreosil, St-Gobain)	70	33.3	0.15	~1463	/	
	Si <sub>0.22</sub> Na <sub>0.22</sub> O <sub>0.56</sub>	65.8	45.9	0.261	ND	/	
	Si <sub>0.2</sub> Na <sub>0.27</sub> O <sub>0.53</sub>	60.2	40.8	0.254	ND	/	
	Si <sub>0.28</sub> Na <sub>0.1</sub> O <sub>0.62</sub>	62.4	34.2	0.196	ND	/	
	Si <sub>23</sub> K <sub>4</sub> O <sub>48</sub>	59.9	35.1	0.153	ND	[73]	
	Si <sub>6</sub> K <sub>2</sub> O <sub>19</sub>	57.4	31.2	0.179	ND	[73]	
	Si <sub>17</sub> K <sub>6</sub> O <sub>37</sub>	53.6	30.7	0.188	ND	[73]	
	Si <sub>4</sub> K <sub>2</sub> O <sub>9</sub>	51.2	30.5	0.207	ND	[73]	
	Si <sub>3</sub> K <sub>2</sub> O <sub>7</sub>	46.4	30.2	0.218	ND	[73]	
	Si <sub>2</sub> K <sub>2</sub> O <sub>5</sub>	44.8	33.1	0.266	ND	[73]	
	Si <sub>3</sub> K <sub>4</sub> O <sub>10</sub>	40.8	33.5	0.277	ND	[73]	
	Si <sub>0.27</sub> Na <sub>0.08</sub> Ca <sub>0.03</sub> O <sub>0.62</sub>	67	37.6	0.203	834	[74]	
	Si <sub>0.26</sub> Na <sub>0.1</sub> Ca <sub>0.017</sub> Al <sub>0.013</sub> O <sub>0.61</sub>	68.9	39.9	0.195	785	[74]	
	Si <sub>0.26</sub> Na <sub>0.1</sub> Ca <sub>0.008</sub> Al <sub>0.013</sub> Mg <sub>0.008</sub> O <sub>0.61</sub>	68.3	37.1	0.187	773	[74]	
	Si <sub>0.26</sub> Na <sub>0.1</sub> Al <sub>0.0134</sub> Mg <sub>0.0167</sub> O <sub>0.61</sub>	66.6	34.5	0.174	763	[74]	
	Si <sub>0.252</sub> Na <sub>0.114</sub> Al <sub>0.013</sub> Mg <sub>0.02</sub> O <sub>0.6</sub>	66.0	34.2	0.179	793	[74]	
	Si <sub>0.242</sub> Na <sub>0.11</sub> Al <sub>0.039</sub> Mg <sub>0.065</sub> O <sub>0.6</sub>	67.3	38.1	0.206	795	[74]	
	Si <sub>0.264</sub> Na <sub>0.087</sub> Ca <sub>0.003</sub> Al <sub>0.013</sub> Mg <sub>0.013</sub> K <sub>0.007</sub> O <sub>0.61</sub>	67.2	35.3	0.183	792	[74]	
	Si <sub>0.261</sub> Na <sub>0.087</sub> Ca <sub>0.008</sub> Al <sub>0.013</sub> Mg <sub>0.013</sub> K <sub>0.007</sub> O <sub>0.61</sub>	69	37.2	0.191	807	[74]	
	Si <sub>0.257</sub> Na <sub>0.088</sub> Ca <sub>0.014</sub> Al <sub>0.014</sub> Mg <sub>0.014</sub> K <sub>0.007</sub> O <sub>0.61</sub>	69.9	39.6	0.206	811	[74]	
	Ca <sub>0.5</sub> Ba <sub>0.5</sub> SiO <sub>3</sub>	79.5	61.24	0.268	ND	[75]	
	Ca <sub>0.5</sub> Ba <sub>0.5</sub> Si <sub>2</sub> O <sub>5</sub>	71.4	50.59	0.265	ND	[75]	
	BaSi <sub>2</sub> O <sub>3</sub>	64.1	47.27	0.274	ND	[75]	
	Mg <sub>0.5</sub> Ba <sub>0.5</sub> SiO <sub>3</sub>	79.5	61.24	0.284	ND	[75]	
	Mg <sub>0.25</sub> Ba <sub>0.75</sub> SiO <sub>3</sub>	71.4	54.04	0.28	ND	[75]	
	Obsidian (Greece)	71.5	38.6	0.191	933	/	
	Si <sub>0.25</sub> Na <sub>0.092</sub> Ca <sub>0.035</sub> Mg <sub>0.021</sub> O <sub>0.6</sub> (Planilux, St-Gobain)	72	44.4	0.23	835	/	
Ca <sub>0.1</sub> Mg <sub>0.1</sub> Si <sub>0.2</sub> O <sub>0.6</sub> (Diopside)	100	74.9	0.282	960	[76]		
Alumino-silicates	Na <sub>30</sub> Al <sub>20</sub> Si <sub>75</sub> O <sub>195</sub>	70.9	38.6	0.194	ND	[77]	
	Na <sub>3</sub> Al <sub>5</sub> Si <sub>6</sub> O <sub>21</sub>	77.3	47	0.226	ND	[77]	
	Na <sub>50</sub> Al <sub>20</sub> Si <sub>65</sub> O <sub>185</sub>	67.1	41.1	0.228	ND	[77]	
	Na <sub>5</sub> Al <sub>5</sub> Si <sub>5</sub> O <sub>20</sub>	73.9	43.2	0.215	ND	[77]	
	Na <sub>60</sub> Al <sub>10</sub> Si <sub>65</sub> O <sub>175</sub>	63.4	41.3	0.244	ND	[77]	
	Na <sub>35</sub> Al <sub>35</sub> Si <sub>65</sub> O <sub>200</sub>	71.2	41.8	0.216	ND	[77]	
	E-glass (Saint-Gobain)	72.3	ND	ND	1119	[110]	
	R-glass (Saint-Gobain)	86	ND	ND	1258	[110]	
	S-Glass	88.9	ND	ND	1258	[110]	
	Ca <sub>0.08</sub> Al <sub>0.15</sub> Si <sub>0.15</sub> O <sub>0.62</sub> (Anorthite)	94.3	65.2	0.261	1125	[76]	
	Ca <sub>0.15</sub> Al <sub>0.1</sub> Si <sub>0.15</sub> O <sub>0.6</sub> (Grossular)	91.4	68.9	0.278	1060	[76]	
	Rare-earth	Y <sub>0.75</sub> Al <sub>1.25</sub> O <sub>3</sub>	139	108	0.286	ND	[24]
		Y <sub>0.48</sub> Al <sub>1.52</sub> O <sub>3</sub>	138	110	0.291	ND	[24]
		La-Al-Si-O	110	ND	ND	1143	/
		Yb-Al-Si-O	135	ND	ND	1178	/
		Al <sub>0.286</sub> La <sub>0.114</sub>	118	0.297	97	1113	[25]
		Al <sub>0.25</sub> La <sub>0.15</sub> O <sub>0.6</sub>	123	0.301	103	1116	[25]
Al <sub>0.224</sub> Y <sub>0.163</sub> Si <sub>0.01</sub> O <sub>0.602</sub>		169	0.291	135	1143	[25]	
Al <sub>0.225</sub> Y <sub>0.146</sub> Si <sub>0.021</sub> O <sub>0.604</sub>		151	0.292	121	1147	[25]	
Al <sub>0.217</sub> La <sub>0.087</sub> Y <sub>0.043</sub> Si <sub>0.043</sub> O <sub>0.609</sub>		126	0.3	105	1121	[25]	
Si <sub>0.093</sub> Al <sub>0.128</sub> Be <sub>0.098</sub> O <sub>0.579</sub>		144.8	ND	ND	ND	[28]	
Si <sub>0.097</sub> Al <sub>0.109</sub> Ti <sub>0.036</sub> Mg <sub>0.079</sub> Zr <sub>0.006</sub> Y <sub>0.061</sub> O <sub>0.579</sub>		139.2	ND	ND	ND	[28]	
Other pure oxides		As <sub>2</sub> O <sub>3</sub>	11.9	11.02	0.32	434	[66]
	TeO <sub>2</sub>	50.7	31.3	0.23	593	[66]	
Oxynitrides	La-Mg-Si-O-N (15 at% N)	133	ND	ND	1111	[53]	
	Lu-Mg-Si-O-N (15 at% N)	146	ND	ND	1138	[53]	
	Ca <sub>0.103</sub> Si <sub>0.207</sub> Al <sub>0.069</sub> O <sub>0.62</sub>	86.2	60.1	0.27	ND	[36]	
	Ca <sub>0.12</sub> Si <sub>0.24</sub> Al <sub>0.02</sub> O <sub>0.605</sub> N <sub>0.015</sub>	93.5	54.5	0.24	ND	[36]	
	Ca <sub>0.117</sub> Si <sub>0.23</sub> Al <sub>0.037</sub> O <sub>0.578</sub> N <sub>0.037</sub>	95.5	65.9	0.28	ND	[36]	
	Ca <sub>0.107</sub> Si <sub>0.214</sub> Al <sub>0.071</sub> O <sub>0.542</sub> N <sub>0.066</sub>	106	70.9	0.265	ND	[36]	
	Y <sub>0.085</sub> Si <sub>0.175</sub> Al <sub>0.106</sub> O <sub>0.635</sub>	122	ND	ND	ND	[45]	
	Y <sub>0.086</sub> Si <sub>0.176</sub> Al <sub>0.107</sub> O <sub>0.61</sub> N <sub>0.021</sub>	132	ND	ND	ND	[45]	
	Y <sub>0.086</sub> Si <sub>0.178</sub> Al <sub>0.108</sub> O <sub>0.584</sub> N <sub>0.043</sub>	144	ND	ND	ND	[45]	
	Y <sub>0.088</sub> Si <sub>0.182</sub> Al <sub>0.11</sub> O <sub>0.53</sub> N <sub>0.088</sub>	158	ND	ND	ND	[45]	

Table I. Continued

Chemical systems	Glass composition	$E$ (GPa)	$K$ (GPa)	$\nu$	$T_g$ (K)	References
	$Y_{11.9}Si_{17.8}Al_{6.8}O_{63.5}$	128	97.0	0.28	1173	[40]
	$Y_{12.3}Si_{18.5}Al_{7.0}O_{54.7}N_{7.5}$	150	119.0	0.29	1183	[40]
	$Y_{12.5}Si_{18.8}Al_{7.2}O_{50.3}N_{11.2}$	165	131.0	0.29	1233	[40]
	$Y_{0.146}Si_{0.232}Al_{0.034}O_{0.31}N_{0.29}$	183	138.6	0.28	ND	[32]
	$Y_{4.86}Mg_{6.3}Si_{16.2}Al_{11.8}O_{54.9}N_{5.92}$	134	101.5	0.28	1118	[78]
Oxycarbides	$SiC_{0.33}O_{1.33}$	104	ND	ND	~1600	[56,57]
	$SiC_{0.375}O_{1.25}$	110	ND	ND	ND	[56]
	$SiC_{0.5}O_{1.24}$	97.9	ND	ND	ND	[55]
	$SiC_{0.8}O_{1.6}$	101	43	0.11	ND	[59]
Metallic/BMGs	$Zr_{55}Cu_{30}Al_{10}Ni_5$	81.4	113.1	0.38	683	/
	$Zr_{41}Ti_{14}Cu_{12.5}Ni_{10}Be_{22.5}$	101	112	0.35	623	[17,79]
	$Gd_{36}Y_{20}Al_{24}Co_{20}$	62.2	57.4	0.319	603	[79]
	$Pr_{60}Al_{10}Ni_{10}Cu_{20}$	37.17	45.16	0.363	409	[79]
	$Cu_{60}Zr_{20}Hf_{10}Ti_{10}$	101.1	128.2	0.369	754	[79]
	$Pd_{40}Cu_{30}Ni_{10}P_{20}$	98	159.1	0.4	560	[79]
	$Pd_{80}Si_{20}$	70	ND	ND	607	[79]
Metallic/Strip shaped	$W_{46}Ru_{37}B_{17}$	309	ND	ND	1151	[21]
	$Fe_{62}Co_{23}B_{15}$	149	ND	ND	ND	[79]

<sup>†</sup>At 77 K. <sup>‡</sup>Typical compositions for aluminophosphate-based laser glass is:  $P_{110-124}Al_{112-24}K_{26-50}Ba_{0-10}Nd_{0-4}O_{311-387}$ . <sup>§</sup>Typical bioactive glass compositions.  $R$  and  $S$  glasses are stiffer and stronger versions of the  $E$  glass which typically contain ~65%  $SiO_2$ , 25%  $Al_2O_3$ , and 10%  $MgO$ , some other materials being present at impurity levels. ND: non-determined. Stoichiometric compositions as well as  $T_g$  are given when available. Experimental errors are typically  $\sim \pm 0.1$  GPa and  $\pm 1$  K for the elastic moduli and the glass transition temperature, respectively. The absence of reference number in the last column means that data were obtained by the present author.

treme thermodynamical conditions (such as high mechanical stresses) existing at sites of large tectonic activity. Basaltic glasses from the anorthite ( $CaAl_2Si_2O_8$ )-diopside ( $CaMgSi_2O_6$ )-forsterite ( $Mg_2SiO_4$ ) system have compositions close to those of the basaltic melts found at volcanic sites and in the oceanic basins.

(H) *Silicon Oxynitride and Oxycarbide Glasses*: Oxynitride and oxycarbide glasses exhibit the highest elastic moduli and glass transition temperature, respectively. In these silicate glasses, oxygen atoms were partially replaced by nitrogen and carbon ones. N and C being threefold and fourfold coordinated, respectively, whereas O is twofold, a significant increase in the atomic network connectivity follows. In oxynitride glasses,<sup>32-53</sup> the largest elastic moduli are reported for those containing alumina and rare-earth oxides (especially  $Y_2O_3$ ,  $Nd_2O_3$ , and  $Lu_2O_3$ ) with up to 15 at.% nitrogen. In contrast to oxynitride glasses, which are generally obtained by means of a conventional melting-quenching-annealing processing cycle, oxycarbide glasses<sup>54-59</sup> are polymer- or gel-derived materials and glasses prepared to date mainly consist of an a- $SiO_2$  matrix with up to 15 at.% covalently bonded carbon forming  $CSi_4$  tetrahedra and some residual free carbon.

(I) *Bulk Metallic Glasses (BMGs)*: Although metallic glasses were discovered in the 1960s, BMGs with specimen thickness larger than 1 mm appeared only about 15 years ago.<sup>17,18</sup> BMGs were obtained in the (Zr,Ti)-(Cu,Ni)-Al-Be systems, using cooling temperature from the melt of the order of  $10^3$  K/s (against  $10^5$ - $10^7$  K/s for the ribbons), by casting of the melt in copper molds. Much different atomic radii are required to favor a chemical disorder. Successfully prepared compositions usually include a metal (Be, Al, ...), a transition metal from the right-hand side of the periodic table (Cu, Ni, ...), a transition metal from the left-hand side (Zr, Ti, Hf, Nb, ...), and a metalloid. Note that data regarding metallic glasses in Fig. 1 were limited to bulk glasses.<sup>20,22</sup>

## (2) Young's Modulus and Glass Transition Temperature

Young's modulus is by far the most frequently reported elastic characteristic and most data in Fig. 1 were obtained by means of USE using piezoelectric transducers (Panel A)<sup>1</sup> or to a lesser extent by other techniques such as Brillouin scattering (BS) (see

for instance Vacher and Boyer,<sup>111</sup> Ecolivet<sup>112</sup>), or mechanical vibration for instance. The estimation of  $E$  from indentation experiments is not straightforward. A reduced Young's modulus,  $E_r = E/(1-\nu^2)$ , is obtained and Young's moduli data derived from indentation methods mostly assume arbitrary values for  $\nu$  and were thus excluded. The glass transition is located at the frontier between the glassy solid state and the supercooled liquid state.  $T_g$  is an essential thermo-physical property of glass.  $T_g$  is mostly estimated by means of differential scanning calorimetry (DSC), where it shows up through an endothermal variation reflecting a change of the thermal capacity, or by means of dilatometry where  $T_g$  is conventionally estimated by intersecting the quasi-linear slopes (in the vicinity of the transition) of the glass and liquid thermal expansion regimes.  $T_g$  of amorphous ice, as detected by a more or less sudden increase in heat capacity during heating (DSC experiments), is not easy to detect and is between 120 and 160 K.<sup>60,105</sup> Most experimental observations suggest  $T_g \sim 136$  K.  $T_g$  of a- $SiO_2$  and silicon oxycarbide glasses were derived from viscosity measurements, using the conventional assignment of  $T_g$  to viscosity between  $10^{12}$  and  $10^{12.6}$  Pa·s.<sup>57</sup>

It is noteworthy that the highest values for  $E$  are not reported for the most refractory glasses (SiOC glasses). This is because SiOC glasses, like a- $SiO_2$ , are characterized by a low atomic packing density, as will be further discussed. Conversely, the high packing density of metallic glasses counterbalances their low bonding energy. Therefore, contrary to the common idea that  $E$  scales with  $T_g$ , which is roughly the case at first sight, it turns out that one can easily find glasses with very different  $T_g$  temperatures exhibiting the same value for  $E$ . For instance, the horizontal dashed line in Fig. 1 corresponds to a Young's modulus of  $\sim 70$  GPa and crosses the data of  $Mg_{65}Cu_{20}Y_{15}$ ,  $Pd_{80}Si_{20}$ , WG (standard soda-lime-silica window glass),  $E$ -, and a- $SiO_2$  glasses, although  $T_g$  for these glasses are, respectively, at 420, 607, 835, 1119, and 1463 K (Table I). Elastic moduli depend much on temperature (see Section V) and their values at temperature  $T$  stem both intrinsically from the fine details of the atomic packing and the atomic bonding types and extrinsically from how far the glass transition of the glass is from the actual temperature. There are indeed two ways to meet a specific value for an elastic modulus at a given temperature. The first one consists in playing on the atomic packing density ( $C_g$ ) and the second one on the bond strength. Both appear to be some-

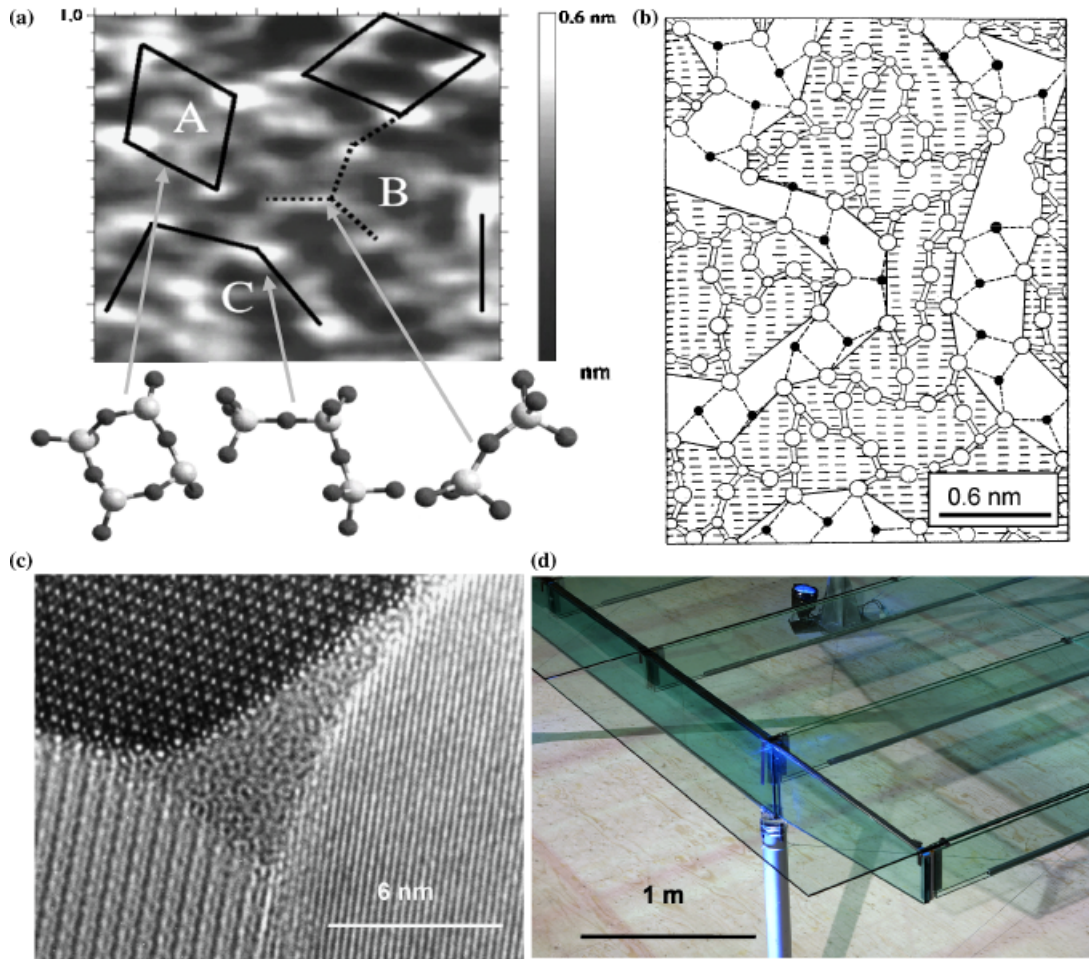


**Fig. 2.** Relevant scales: (a) The atoms and the structural units (here the  $\text{SiO}_4$  tetrahedron) and their possible combinations (atomic force microscopy)— $\alpha\text{-SiO}_2$  case, after Poggemann *et al.*<sup>116</sup>; (b) The supramolecular scale—The modified random network proposed by Greaves<sup>121</sup> and supposing the existence of alkali-rich (solid circles) percolating channels; (c) The long-range scale—Glassy pocket at a triple grain junction in a  $\text{Si}_3\text{N}_4$ -based ceramics, after Rouxel and Wakai<sup>188</sup>; and (d) The macroscopic scale—Here a detail of an “all transparent pavilion,” a window glass frame built on long loaded glass beams for innovative building design.<sup>125</sup>

what interconnected, so that it is difficult to obtain a strong bonding and a high density at the same time. With  $C_g \sim 0.45$ ,  $\alpha\text{-SiO}_2$  is a model example of a low packing density of strongly bonded atoms ( $U_{\text{O-Si-O}} \sim 800$  kJ/mol). Hence, while elastic moduli reflect a mean volume density of energy,  $T_g$  is related to a mean atomic bonding energy regardless of the packing density, so that it increases monotonically as the fraction of weakest bonds decreases to the benefit of stronger ones, consistently with the classical order: van der Waals < metallic < ionic < covalent.

### III. Atomic Organization and Elastic Properties

#### (1) Different Scales of Concern

In order to understand the elastic properties of known glasses or even better, to predict those of glasses that have not been synthesized as yet, it is necessary to study the organization at the atomic scale. Elastic moduli do not solely depend on the interatomic bonding energy but also depend on the coordination, on the polymerization degree (cross linking), on the atomic packing density, and on the molecular organization, including the possible formation of ring, chain, or layer units. This calls for a multiscale approach. At first sight, the four relevant scales of concern are (i) the atomic one, over 1.5–2.5 Å, (ii) the molecular one, from 2.5 to 4.5 Å, (iii) the “network” one, within few nanometers, and (iv) the continuum scale, over a hundred nanometers. These scales are illustrated in Fig. 2. Scales (i) and (ii) are associated to the short- to medium-range order, which can be

studied by nuclear magnetic resonance, Raman scattering spectroscopy, neutron scattering,<sup>113–115</sup> or atomic force microscopy<sup>116</sup> for instance. At the network scale some kind of symmetry shows up beyond the atomic and molecular disorders. Scale (iv) is ruled by standard continuum mechanics equations and extends to the macroscopic scale of the functional components (window, lens, fibers, bottle, balls, flat panel display, etc.).

The “molecular scale”: this scale is the one of the cross linking of the glass network with the occurrence of clusters (dimension 0D), uni- (1D), bi- (2D), or tri-dimensional (3D) units. While there are convincing observations for the existence of clusters with icosahedral-like symmetry in some BMGs,<sup>117,118</sup> clusters are also likely to occur in glassy water<sup>107</sup> as well as in  $\text{As}_2\text{S}_3$  glass for instance (clusters consisting of a hard sphere of  $\text{As}_4\text{S}_6$  molecules).<sup>119</sup> Chains form in pure selenium ( $-\text{Se}-$ )<sub>n</sub>, in metaphosphate such as  $\text{LiPO}_3$  built on  $\text{PO}_3^-$ - $\text{Li}^+$  units, or in  $\text{CaSiO}_3$ . Layer-like units are found in  $\text{P}_2\text{O}_5$ ,  $\text{B}_2\text{O}_3$ ,  $\text{GeSe}_4$ , or  $\text{Si}_2\text{Na}_2\text{O}_3$  glass (which consists of  $\text{SiO}_{5/2}$ - $\text{Na}^+$  units). Glass networks may also contain rings ( $\text{Si}_n\text{O}_n$ ,  $\text{Ge}_n\text{O}_n$ , or  $\text{P}_n\text{O}_n$  rings where  $n \sim 6$ , boroxol rings in borates or  $\text{Se}_8$  rings in  $\alpha\text{-Se}$ ). This cross linking greatly affects  $E$  and  $T_g$ . In the Ge–Se system,  $T_g$  and  $E$  increase almost linearly with the Ge content whereas  $U_{\text{O-Ge-Ge}} < U_{\text{O-Ge-Se}}$  and  $U_{\text{O-Ge-Ge}} < U_{\text{O-Se-Se}}$ . This trend stems from the change in the molecular architecture or in the medium-range network topology. Fourfold coordinated Ge atoms increase the cross-linking degree and network dimensionality. The glass network evolves from a mixture of chain-like units to a mixture of layer-like units and further to a 3D organization. With regard to pure Se glass consisting of chains and possibly of rings, with  $T_g = 313$  K and

$E = 10.2$  GPa, the  $\text{Ge}_{0.4}\text{Se}_{0.6}$  glass exhibits much better properties:  $T_g = 613$  K and  $E = 22.4$  GPa.<sup>14</sup> In the case of glasses with covalently bonded elements, the mean coordination number ( $\langle n \rangle$ ) is a useful tool to correlate the physical properties to the structural changes.  $\langle n \rangle$  is defined as  $\langle n \rangle = \sum_i f_i n_i$  where  $f_i$  and  $n_i$  are the atomic fraction and the coordination number of the  $i$ th constituent, respectively. For example, for a  $\text{Ge}_x\text{Se}_{1-x}$  ( $x \leq 1$ ) glass, this number writes  $\langle n \rangle = 2(x+1)$ . As far as  $\langle n \rangle$  is  $< 2.1$ , the volume fraction of Ge-containing chains is negligible so that deformation essentially proceeds through the alignment of the chains with the main loading axis in tension or in transverse planes in compression. In this case properties are mainly governed by the weak interchains van der Waals forces. A low shear resistance and a high Poisson's ratio follow. As  $\langle n \rangle$  increases, covalent bonds come into play.  $\langle n \rangle = 2.4$  ( $\text{GeSe}_4$  composition) corresponds to a complete cross linking of Se and Ge layer units, two neighboring Ge atoms being separated by two Se atoms. At  $\langle n \rangle = 2.67$  ( $\text{GeSe}_2$  stoichiometry), Ge-Ge starts to form and a 3D network builds up, leading to a significant increase of  $E$  and  $T_g$ . A comparable situation exists in borate glasses. In this latter case, the stiffness predicted from the interconnected layers of  $\text{BO}_3$  triangles is greatly overestimated due to the presence of weak interlayers bonds. For oxide glasses, the number of bridging oxygen atoms per glass-forming cation (Si, Al, Zr, As, B, P, etc.),  $n_{\text{BO}}$ , provides a measurement of the network cross-link degree. This number is defined as  $n_{\text{BO}} = 4 - \sum_i M_i z_i / (\sum_j F_j)$  where  $M_i$  and  $z_i$  are the atomic fraction (after deduction of the number of charge compensators) and the valency of the  $i$ th modifying cation and  $F_j$  is the fraction of the  $j$ th glass-forming cation. For pure oxide glasses such as  $\text{As}_2\text{O}_3$ ,  $\text{B}_2\text{O}_3$ , and  $\text{P}_2\text{O}_5$ ,  $n_{\text{BO}} = 3$  and  $v \approx 0.3$ , whereas for a- $\text{SiO}_2$  and a- $\text{GeO}_2$ ,  $n_{\text{BO}} = 4$  and  $v < 0.2$ . For a  $(\text{SiO}_2)_w(\text{Al}_2\text{O}_3)_x(\text{CaO})_y(\text{Na}_2\text{O})_z$  glass, assuming all Al atoms are fourfold coordinated, this number is given by  $n_{\text{BO}} = 4 - 2(y+z-x)/(w+2x)$ . An extension to the cases of oxycarbide and oxynitride glasses is obtained by replacing [O] by an equivalent anionic concentration  $[\text{O}^*]$ , with  $[\text{O}^*] = [\text{O}] + 3/2[\text{N}] + 2[\text{C}]$ . Nuclear magnetic resonance measurements lead mostly to experimental  $n_{\text{BO}}$  values very close to the theoretical ones. Oxynitride and oxycarbide glasses provide a good illustration of the impact of the glass network cross-linking degree on the elastic moduli. These glasses are stiffer and more refractory than their parent oxide glasses (same cationic species). However, the values for the bonding energies do not corroborate this tendency:  $U_{\text{O-Si-C}} (447 \text{ kJ/mol}) \approx U_{\text{O-Si-N}} (437 \text{ kJ/mol}) < U_{\text{O-Si-O}} (800 \text{ kJ/mol})$ . Photoelectron spectroscopy (XPS) measurement on Si confirmed the presence of lower energies (Fermi levels) in oxycarbide environments than in oxide ( $\text{SiO}_2$ ) ones.<sup>120</sup> Hence, similar to what governs the rigidity of steel frames, the source for the excellent stiffness of oxynitride and the good one of oxycarbide glasses lies in the 3D bonding architecture rather than in the bond strength itself. Note, however, that this reasoning may be greatly complicated in some cases due to possible phase separations (chain-forming chalcogen atoms tend to stay together in chalcogenide glasses) or clustering (including rings). Remark also that  $\langle n \rangle$  and  $n_{\text{BO}}$  are not equivalent parameters. For instance, in the case of a- $\text{SiO}_2$ ,  $\langle n \rangle = 2.67$  whereas  $n_{\text{BO}} = 4$ .

(A) *Mesoscopic or "Supramolecular" Scale:* A glass is a solid with a small length of coherency, with respect to optical wavelengths for instance. However, in most glasses, including metallic ones, few nanometer large nano-domains seem to exist. Glasses would hence possess some organization at a mesoscopic scale. Even though this latter scale is partly experimentally accessible by means of X-ray absorption spectroscopy (EXAFS),<sup>121</sup> neutron diffraction,<sup>122</sup> or by low-frequency Raman scattering,<sup>122-124</sup> it still remains poorly understood. The size of the "domains," which are likely to be amorphous, is typically  $< 10$  nm and can be estimated from the frequency of the "Boson" peak observed in the  $3-50 \text{ cm}^{-1}$  Raman frequency range. The estimated correlation lengths, in good agreement with first diffraction peak measurements, are much larger than the characteristic distances of the short-range order. In the light of these investigations, glass appears as a nano-composite material consisting of islands immersed in a more-easily deformable

softer phase and this has to be considered to discuss the elastic behavior, especially at high temperatures (see Section V(4)).

(B) *Macroscale:* Although there is a growing number of examples of large loaded glass structures such as free-form glass domes, cable net walls, glass beams, glass fins, and glass columns, general rules for the elastic stability (lateral torsional buckling for instance) and for the safety of the glass structural design are still missing. Besides, the transition from the lower end of the continuum scale ( $\sim 10$  nm) to the macro-scale still raises major technological difficulties among which are (i) the unavailability of glass sheets and profiles with large (beyond standards) dimensions; (ii) the edge defects sensitivity (flaw tolerancy); and (iii) the risk for lateral torsional buckling stemming from the use of large but thin glass sheets. However, glasses possess a unique combination of physical properties (for instance in the case of soda-lime-silica: transparency, intrinsic strength, stiffness, lightness, and availability of relatively low-cost raw materials), which, besides esthetics, makes this peculiar material very promising for civil engineering and attractive for architects and designers.<sup>125-127</sup>

## (2) Atomic Bonding and Packing Density

The elastic properties depend much on the chemio-physical properties of the interatomic bonds. Unfortunately, fundamental characteristics such as the interatomic distance ( $d$ ) and the directionality or the coordinence ( $n$ ) of every atom in its current situation in the glass are usually not accurately known. Under such circumstances, bonding energies<sup>109,128</sup> and cationic field strength are mostly roughly estimated and can only give tendencies within given glass systems. Besides, based on a purely electrostatic interaction, the field strength approach suits quite well oxide glasses but becomes more and more questionable as the covalency of the interatomic bonding increases, such as in nitride and carbide systems. The situation is even more complex when weak van der Waals-type bonds coexist with strong covalent bonds, as in chalcogenide glasses.

Another major parameter is the glass atomic packing density ( $C_g$ ), defined as the ratio between the minimum theoretical volume occupied by the ions and the corresponding effective volume of glass:

$$C_g = \rho \sum f_i V_i / \sum f_i M_i \quad (1)$$

with for the  $i$ th constituent with  $A_x B_y$ , chemical formula:  $V_i = 4/3\pi N (x r_A^3 + y r_B^3)$ , where  $\rho$  is the specific mass,  $N$  is the Avogadro number,  $r_A$  and  $r_B$  are the ionic radii,  $f_i$  is the molar fraction, and  $M_i$  is the molar mass.<sup>128</sup> The effective ionic radii in glass are usually not known with high accuracy. Shannon<sup>129</sup> tabulated the crystal radius and the effective ionic radius of halides and chalcogenides (including oxides). Whittaker and Muntz<sup>130</sup> suggested to use the mean of both values in the case of silicate glasses.

For instance,  $C_g$  is about 0.52 for a standard window glass and 0.45 for a- $\text{SiO}_2$ . An estimation of the packing density in metallic glasses was obtained by giving the atomic radius of each element its value in the corresponding pure metal. High-pressure experiments ( $P > 15$  GPa) and numerical simulations on disordered packings seem to indicate that maximum expected  $C_g$  values are about 0.65, whereas ordered systems may reach the theoretical value of 0.74 corresponding to face-centered cubic structures.<sup>131,132</sup> Note, however, that relatively high values ( $> 0.75$ ) are obtained for multicomponent (mixtures of small and large atoms) metallic glasses, consistently with the remarkably high elastic moduli of these glasses.

Both interatomic energies ( $U_o$ ) and atomic packing densities have to be taken into account to interpret elasticity data. For example, the substitution of Ca by Mg in a soda-lime-silica glass with 78 mol%  $\text{SiO}_2$  and 15 mol%  $\text{Na}_2\text{O}$  does not lead to a stiffness increase as would be anticipated from the values of the bonding energies ( $U_{\text{O-Mg-O}} > U_{\text{O-Ca-O}}$ ): both  $T_g$  and  $E$  decrease, from 785 to 773 K and from 69 to 66 GPa, respectively.<sup>74</sup> This is due to a significant decrease of  $C_g$ , from 0.487 to 0.482. The

same explanation holds for the decrease of the stiffness observed in the same glass system when Mg is replaced by Si. Although  $U_{\text{Si-O}} > U_{\text{Ca-O}} > U_{\text{Mg(VI)-O}} > U_{\text{Na-O}}$ ,  $C_g$  decreases from 0.491 to 0.484 as the  $\text{SiO}_2$  content increases from 72 to 80 mol%. In the meantime,  $E$  decreases from 70.2 to 65.6 GPa. This simple reasoning can be easily applied to germanate and borate glasses too. The addition of BaO or  $\text{Ga}_2\text{O}_3$  to  $\text{GeO}_2$  significantly improves the stiffness although  $U_{\text{Ga-O}} (374 \text{ kJ/mol}) < U_{\text{Ba-O}} (562 \text{ kJ/mol}) < U_{\text{Ge-O}} (653 \text{ kJ/mol})$ . A similar tendency is observed when  $\text{Na}_2\text{O}$  is added to  $\text{B}_2\text{O}_3$  or  $\text{P}_2\text{O}_5$  although  $U_{\text{Na-O}} (256 \text{ kJ/mol}) < U_{\text{B-O}} (809 \text{ kJ/mol}) < U_{\text{P-O}} (585 \text{ kJ/mol})$ . The immediate consequence is that elastic moduli predictions solely based on the number of nonbridging oxygen in oxide glasses, on the ionic field strength in ionic glasses, or on the atomic network connectivity in strongly covalent glasses (chalcogenide glasses) are questionable simply because these parameters give an incomplete picture of the problem, although apparent simple correlations may be observed through given glass systems or within small network structure perturbations.

Elastic moduli depend simultaneously on the interatomic bonding energy and on the atomic packing density. Both ingredients are included in the expression for the bulk elastic modulus ( $K$ ), which derives from the form of the interatomic potential. In the simplistic case of a Lennard-Jones-type potential, it comes (first Grüneisen rule)<sup>133</sup>:

$$K = V_o \left. \frac{\partial^2 U}{\partial V^2} \right|_{V_o} = \frac{mn}{9V_o} U_o \quad (2)$$

where  $U_o$  is the atomic bonding energy,  $V_o$  is the atomic volume at equilibrium, and  $m$  and  $n$  are the exponents of the power law describing the attractive and the repulsive terms, respectively.

### (3) *Ab-Initio Estimation of the Elastic Moduli*

In an early study published in 1894 by Winkelmann and Schott,<sup>80</sup> a linear dependence was proposed between  $E$  and the glass composition. Interestingly, the obtained weighting coefficients revealed a stronger effect for  $\text{Na}_2\text{O}$  (98.1), CaO (98.1), or  $\text{K}_2\text{O}$  (69.7) than for the major glass former  $\text{SiO}_2$  (63.8), where the molar fraction of each oxide is weighted by the coefficients in the brackets (the resulting Young's modulus is expressed in GPa). Coefficients of 157 and 19.6 were attributed to glass formers such as  $\text{Al}_2\text{O}_3$  and  $\text{B}_2\text{O}_3$ , anticipating what we know today: Boron in  $\text{B}_2\text{O}_3$  forms relatively weakly bonded together  $\text{BO}_3$  triangles, whereas Al acts as a 3D glass former, mainly fourfold coordinated but allowing for a better atomic packing density than Si. These results already support the fact that it is necessary to fill the space in the a- $\text{SiO}_2$  network by means of nonglass-forming cations, thus enhancing the atomic packing density, to reach large values for the elastic moduli. The relative error of the prediction was always  $< 8\%$  and typically  $\sim 4\%$ . For instance, for a standard window glass (say 71%  $\text{SiO}_2$ , 13%  $\text{Na}_2\text{O}$ , 10% CaO, and 6% MgO) this gives  $E = 71.4 \text{ GPa}$  (72 GPa experimentally). Following this empirical approach, Phillips<sup>83</sup> and Williams and Scott<sup>84</sup> proposed refined series of coefficients leading to a better than 0.13% estimation of Young's modulus among large sets of silicoaluminate glasses. However, unexplained discrepancies showed up in some chemical systems, which called for a better understanding of the glass structure.

It appears from Eq. (2) that  $K$  is proportional to a volume density of energy. In the case of glasses, neither the atomic volumes nor the bonding energy are accurately known. Furthermore,  $m$  and  $n$  depend on the chemical nature of the bonds and are likely to fluctuate with the composition. Nevertheless, the former expression gave birth to several theoretical models aimed at providing *ab initio* values for the elastic moduli, with excellent results in the case of diamond and zinc-blende solids and reasonable agreement in the case of oxide glasses.<sup>38,70,85</sup> The most widely used model is the one proposed by Makishima and Mackenzie,<sup>70</sup> hereafter referred to as MM's model, which expresses  $E$  as a function of the volume density of energy,  $\Delta H_{ai}^V$ ,

and  $C_g$

$$E = 2C_g \sum f_i \Delta H_{ai}^V \quad (3)$$

where the volume energy density of the  $i$ th oxide is calculated from the molar dissociation (or atomization) energy ( $\Delta H_{ai}$ ), from the molar mass ( $M_i$ ), and from the density of the oxide ( $\rho_i$ ):  $\Delta H_{ai}^V = \rho_i / M_i \times \Delta H_{ai}$ . Although the theoretical prediction of  $E$  as well as the tendencies through series of silicate glasses are quite satisfactory, the elastic moduli of phosphate and borate glasses are greatly overestimated. In phosphates, this is due to the presence of double  $\text{P}=\text{O}$  bonds, which do not contribute to the network stiffness (the oxygen atom is not bridging), so that the corresponding energy should be subtracted from the dissociation energy of the  $\text{P}_2\text{O}_5$  compound. In borates, the overestimation originates from the weak bonds between the planar  $\text{BO}_3$  triangle (to be compared with the  $\text{B}_2\text{O}_3$  crystal built on  $\text{BO}_4$  units). On the contrary,  $E$  is greatly underestimated (by over 20%) in the case of germanate, aluminate, and high-modulus glasses in general (beryllium- and nitrogen-containing glasses for instance), and when a relatively good correspondance is noticed between theoretical and experimental data, opposite trends are sometimes observed. Some refinement was proposed by Rocherullé *et al.*<sup>38</sup> in the case of oxynitride glasses. However, the poor knowledge of the actual ionic radii and coordination number for each ion in a glass network as well as the wide range of glass systems and the correlative structural diversity make rather hopeless the finding of a universal expression for the elastic moduli chiefly based on the properties of the individual constituents. Furthermore, such theoretical calculation requires the actual value for the glass density (see Eq. (1) for  $C_g$ ), so that the *ab initio* character is somewhat lost. As was recently underlined by Daucé *et al.*,<sup>47</sup> a reliable quantitative estimation based on the MM-type approach is only possible for glasses with compositions close to those of crystallized compounds for which the actual ionic radii are accurately known. Furthermore, the dissociation energy is not a reticular energy and it is not obvious that  $C_g$  can be used as an ersatz of the Madelung constant.

Let us come back to Eq. (2) and examine the dependence of  $K$  on the atomization (dissociation) enthalpy, which is a measurement of the mean atomic network energy. For a multi-constituent glass this enthalpy can be roughly estimated from the properties of the constituents according to:

$$\left\langle \frac{U_o}{V_o} \right\rangle = \sum f_i \Delta H_{ai} / \left( \sum f_i M_i / \rho_i \right) \quad (4)$$

where  $\rho_i$  is the specific mass,  $f_i$  and  $M_i$  are the molar fraction and the molar mass, respectively, with for the  $i$ th constituent written  $\text{A}_x\text{B}_y$ , according to an ordinary Born-Haber cycle:

$$\Delta H_{ai} = x\Delta H_f^\circ(\text{A}, g) + y\Delta H_f^\circ(\text{B}, g) - \Delta H_f^\circ(\text{A}_x\text{B}_y) \quad (5)$$

The standard formation enthalpy of a cation is equal to its sublimation enthalpy whereas for an anion gaseous in its standard state, the molar dissociation energy of the gas molecules must be considered. The denominator in the right-hand side in Eq. (4) represents the whole volume occupied by the atoms of an "equivalent" mole of glass, provided the volume occupied by each atom is the same as in the crystal of the raw material introduced during the synthesis. The presence of free volume in the glass and therefore of an atomic packing density lower than the one of a crystallized solid with the same composition is thus not taken into account in this *ab initio* approach. We will see further that the advantage of doing so is that discrepancies between theoretical and experimental  $K$  values shed some light on the actual atomic packing. In the case of  $\text{SiO}_{1.6}\text{C}_{0.8}$ , because there are no thermodynamics data for the actual processing method, the dissociation energy was estimated assuming a synthesis from SiC (12.5%),  $\text{SiO}_2$  (0.5%), and C (0.375%) whereas

a polymer route leaving some free carbon in the material was used. For the residual carbon an intermediate density between the ones of graphite and diamond was chosen. In the case of chalcogenide glasses little information was available regarding the thermodynamics of the studied compositional systems. Shkol'nikov<sup>134</sup> proposed an estimation from the atomic bonding energies and coordination numbers

$$\Delta H_{ai} = N \langle U_o \rangle \langle n_c \rangle \quad (6)$$

where  $\langle U_o \rangle$  and  $\langle n_c \rangle$  are the mean covalent bonding energy and the average number of covalent bonds per atom, respectively. This number  $\langle n_c \rangle$  turns out to be half the mean coordination number:  $\langle n_c \rangle = \langle n \rangle / 2$ . For instance, for  $\text{GeSe}_4$  glass  $\langle U_o \rangle = 1/3(U_{\text{OSe-Se}} + 2U_{\text{OGe-Se}})$  and  $\langle n_c \rangle = 6/5$ . In cases where the actual formation enthalpies were available,<sup>135</sup> the above method (Eq. (6)) appears to significantly underestimate the volume density of energy.

Most experimental  $K$  data increase monotonically with the volume density of energy (Fig. 3). However, there are several opposite tendencies and in all cases the slopes depend much on the glass chemical system. Previous investigators attempt to refine the MM model to obtain a better matching between experimental data and theoretical results. Nevertheless, the *ab initio* data obtained on the basis of Eq. (4) reveals interesting features that can be tentatively related to details of the atomic network structure. The case of borates was already interpreted by Makishima and Mackenzie<sup>70,85</sup> as the evidence for an increasing fraction of weakly bonded-together planar  $\text{BO}_3$  triangle units with increasing alkaline content in the glass. Because the calculation is performed with data obtained from crystallized  $\text{B}_2\text{O}_3$ , which is built on 3D cross-linked units (trigonal structure), the energy density is more and more overestimated when rising  $\text{Na}_2\text{O}$  fraction. In the case of chalcogenide glasses, it is noteworthy that van der Waals bonds are usually systematically ignored in the theoretical models developed so far (most of which are based on the average coordination number), either to analyze the structural organization or to relate composition to elastic properties. However, these relatively weak bonds are expected to play a major role, especially for chalcogen-rich compositions, such as the hydrogen bond in the case of glassy ice. This is presumably why the calculated energy density seems greatly overestimated in these latter glasses (Fig. 3). Besides the bonding characteristics, the atomic packing density is another important ingredient governing the elastic moduli. The energy data in Fig. 3 were obtained from the properties of crystallized phases. There are obvious packing density differences between the glass and the mother materials (starting powders). We will show in the next paragraph that unlike elastic moduli that combine energy and packing density, Poisson's ratio is a direct indicator of the atomic packing density.

At first sight the increase of the elastic moduli with increasing Al content in aluminosilicates is surprising because the Al–O bond (502 kJ/mol) is much weaker than the Si–O one ( $\sim 800$  kJ/mol). But in comparison with silicon, aluminum favors structural disorder and thus the addition of alumina leads to an enhancement of  $C_g$ , which compensates the decrease in bonding energy. Al is sixfold coordinated in  $\alpha$ -alumina, whereas it is mainly fourfold coordinated in aluminosilicate glasses. As a result, the atomic packing density is smaller in aluminosilicate glasses (around 0.48 in sodium–aluminosilicates<sup>77</sup>) than in the crystallized counterparts ( $C_g \sim 0.75$  for  $\alpha\text{-Al}_2\text{O}_3$ ) and the calculated energy density lies above the actual value for the bulk modulus. Nevertheless, at relatively high alumina content, five- and sixfold-coordinated Al show up<sup>136–139</sup> and  $C_g$  increases.  $C_g$  reaches  $\sim 0.55$  in  $\text{Y}_2\text{O}_3\text{-Al}_2\text{O}_3$  glasses, which possess a bulk moduli of  $\sim 110$  GPa.<sup>24</sup> All these structural considerations are consistent with the data plotted in Fig. 3.  $K$ ,  $\langle U_o/V_o \rangle$ , and  $K/\langle U_o/V_o \rangle$  increase monotonically with the Al content. This latter parameter indicates that the glass atomic packing density gets closer to the one of the crystallized counterparts.

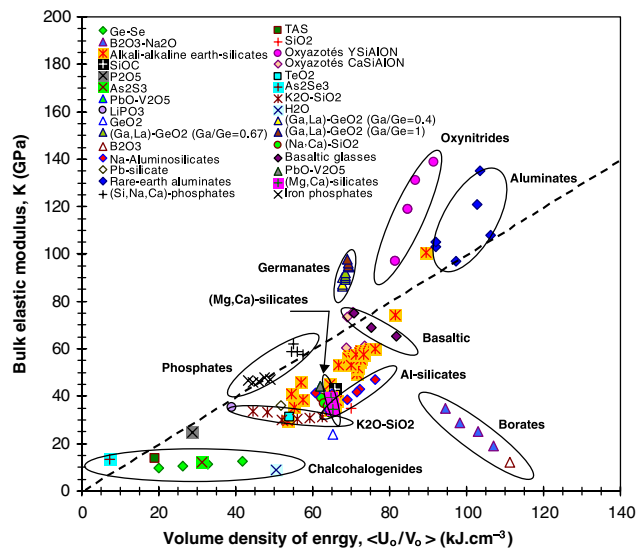


**Fig. 3.** Experimental bulk modulus as a function of the calculated volume density of energy (from the physical and thermodynamical properties of the raw materials).<sup>128,135</sup> The dashed line corresponds to  $K = \langle U_o/V_o \rangle$ , i.e., to  $m = 1$  (Coulombian attraction) and  $n = 9$  in Eq. (2). This line separates glasses with high atomic packing density and bonding energy (above) from those with low atomic packing density and relatively weak interatomic bonds (below).

In comparison with the silicoaluminates, the situation in germanate glasses is reverse. The energy density calculation is made from available thermodynamics data for the quartz form of germania, whose structure is hexagonal with three  $\text{GeO}_2$  molecules per unit cell. Contrary to this structure, characterized by a  $\text{GeO}_4$  tetrahedral framework,  $\text{GeO}_5$  and  $\text{GeO}_6$  polyhedra predominate in alkali-germanate glasses<sup>100,101</sup> and may be largely present in (La, Ga)-germanate glasses too.<sup>69</sup> Consequently,  $C_g$  is probably higher in the glass than expected from the constituents and  $K \gg \langle U_o/V_o \rangle$ . The steep slope associated with the germanate data in Fig. 3 suggests that the Ge atom environment is very sensitive to the glass composition. The position of  $\alpha\text{-GeO}_2$  in Fig. 3, well below the line corresponding to  $K/\langle U_o/V_o \rangle = 1$ , further reflects the rather open structure (low  $C_g$ ) of this pure oxide glass, which is likely to resemble that of  $\alpha\text{-SiO}_2$ .

The case of magnesium is interesting because when Mg replaces Ca in silicates (see for instance the S1 to S3 compositions in Deriano *et al.*<sup>74</sup> where the  $\text{MgO}/\text{CaO}$  ratio is increased while keeping the  $\text{MgO}+\text{CaO}$  content at 5 mol% in a series of  $\text{SiO}_2(78)\text{-Na}_2\text{O}(15)\text{-Al}_2\text{O}_3(2)\text{-MgO-CaO}$  glasses), the elastic moduli decrease (for instance  $K$  decreases from 40 to 34.5 GPa when MgO increases from 0 to 5 mol%<sup>74</sup> although Mg–O and Ca–O bond strengths are very close and although  $\langle U_o/V_o \rangle$  is found to increase (an increase is also predicted with the MM's model). The cationic field strength is even higher for Mg than for Ca and both cations have the same valency. The reason for this discrepancy is that Ca is mostly eightfold coordinated whereas Mg is sixfold so that Mg decreases the atomic packing density. A similar anomaly is observed in (Mg or Al)-Ca-rich basaltic glasses.

The way alkaline ions affect  $C_g$  in borate, germanate, phosphate, and silicate glasses was discussed in details by Giri *et al.*<sup>140</sup> The important finding is that in all cases  $C_g$  increases rapidly with the alkaline content up to  $\sim 50$  mol% and that large alkali are more efficient than small ones ( $\text{Cs} > \text{K} > \text{Na} > \text{Li}$ ) for enhancing  $C_g$ . However, the resulting decrease of the bonding energy may counterbalance the gain in packing density, as in the case of  $\text{K}_2\text{O-SiO}_2$  glasses for  $\text{K}_2\text{O}$  contents lower than 25%. At larger fractions of alkaline, the bulk modulus is found experimentally to increase, although the theoretical calculation predicts a decrease (Fig. 3).

Despite the simple tendencies observed within limited compositional changes, there is no general correlations between the

elastic moduli, the fraction of nonbridging anions, the glass transition temperature, or the glass network connectivity.

**(4) Poisson's Ratio, Atomic Packing Density, and Network Dimensionality**

Poisson's ratio is the negative of the ratio of transverse contraction strain to longitudinal extension strain in the direction of elastic loading (Panel B). Hence,  $\nu$  reflects the resistance of a material opposes to volume change with respect to shape change and is small for shear-resistant compressible materials, such as cellular solids,<sup>141</sup> but tends toward 0.5 for incompressible bodies such as rubber. Although the theory of isotropic elasticity allows  $\nu$  values between  $-1$  (negative values are found at low strain in some polymeric foams<sup>142</sup>) and 0.5, most familiar materials have Poisson's ratio close to 0.3 so that relatively little attention is paid to the actual value for  $\nu$  (Poisson himself thought his ratio was constant and equal to 0.5).<sup>143</sup> However, glasses exhibit a wide range of values for  $\nu$  from 0.1 to 0.4, which correlate with the glass network polymerization degree, hence reproducing at the atomic scale what is observed in cellular materials at the macroscopic scale.<sup>66,144,145</sup>

The molecular scale governs the glass network compactness and dimensionality. Poisson's ratio plays here a very interesting role and it is quite unfortunate that most reported studies were limited to Young's modulus. It seems indeed that the knowledge of  $\nu$  suffices to evaluate  $C_g$  (Fig. 4) and to estimate the network dimensionality (Fig. 5). Although  $C_g$  values cannot be accurately measured, mainly because of the lack of actual atomic radius data (provided it has a meaning), the wide spectrum of glasses investigated in this review, with different types of atomic bonds, shows a clear trend:  $C_g$  increases monotonically with  $\nu$ , from about 0.41 for an SiOC glass ( $\nu = 0.11$ ) to about 0.87 for a PdCuNi glass ( $\nu = 0.4$ ). This tendency is also observed within given chemical systems. For instance, in alkali silicates  $\nu$  increases with the alkali contents as the atomic packing density increases.<sup>73,88</sup> In alkali-aluminosilicate glasses, with increasing aluminum content Al coordination changes from 6 (small Al quantities) to 4 (Al is network forming) and further to 5 and 6 when there are no longer enough alkali ions to balance the excess negative charge within  $AlO_4$  tetrahedra (for instance when  $Al_2O_3/Na_2O > 1$ ).<sup>136,139</sup> As a network former Al decreases the atomic packing density, whereas in comparison  $C_g$  is enhanced by sixfold network modifying Al atoms. Consequently,  $\nu$  exhibits a slight increase at low Al contents, then a steep decrease up to  $Al_2O_3/Na_2O = 1$  and a regain at higher Al contents.<sup>77</sup> The same reasoning holds for (Mg,Ca)-aluminosilicates: When Ca atoms are replaced by smaller and lighter Mg atoms or when Mg substitutes for Si,  $C_g$  increases (although the glass density may decrease) and so does  $\nu$ .<sup>74,103</sup> At first glance, a linear dependence may be observed between  $\nu$  and  $C_g$  for glasses belonging to similar systems ( $\nu = 0.5 - 1/7.2C_g$  was proposed by Makishima and Mackenzie<sup>85</sup>). However, a global overview (Fig. 4) reveals a more complicated sigmoidal-like trend. Interestingly, carbon steels, with Poisson's ratio ranging between 0.29 and 0.33 and compactness between 0.68 (BCC, ferritic steel) and 0.74 (FCC, austenitic steel), would also fit the  $\nu(C_g)$  curve nicely.

Furthermore, Poisson's ratio is correlated to the glass network connectivity. Experimental data show that  $\nu$  decreases monotonically with  $\langle n \rangle$  or  $n_{BO}$  (Fig. 5). A highly cross-linked network, as exemplified by amorphous silica (a-SiO<sub>2</sub>), leads to a small Poisson's ratio ( $\nu = 0.15$ ), whereas weakly correlated networks, such as for chain-based chalcogenide glasses or cluster-based metallic glasses, exhibit values higher than 0.3 (up to 0.4) (Fig. 6). Hence, as it was already noticed by Bridge and Higazy<sup>144</sup> in a study limited to some oxide glasses and later for a wide range of glasses including covalent and metallic ones,<sup>145</sup>  $\nu$  depends on the dimensionality of the structural units. This tendency is even observed within glass series belonging to a given system and is particularly pronounced when elements with very different valencies substitute one for the other, such as in the case of the replacement of twofold Se by fourfold Ge in binary

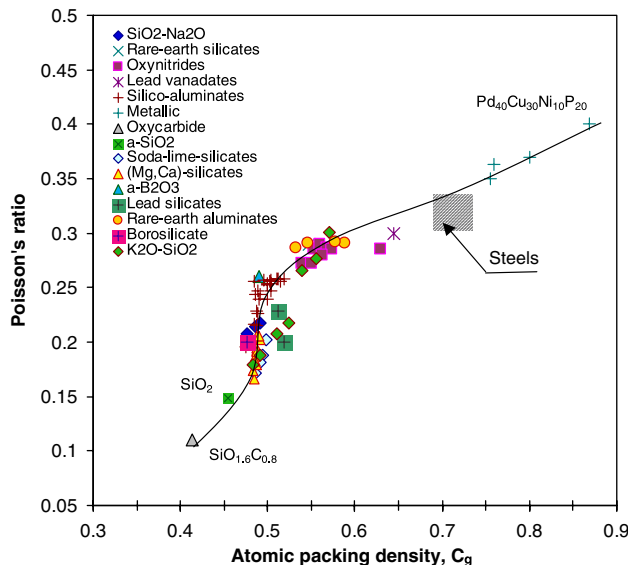


Fig. 4. Poisson's ratio and atomic network packing density.

Ge<sub>x</sub>Se<sub>1-x</sub> glasses<sup>14</sup> or when chalcogen atoms are substituted by atoms with higher coordination numbers in multicomponent chalcogenide glasses,<sup>11</sup> or also when Na(+1) or K(+2) substitutes for Si(4+) in silicate glasses. Conversely,  $\nu$  is little affected by Al(3+) to Si(4+)<sup>77</sup> or Mg(2+) to Ca(2+) substitutions.<sup>103</sup> On the one hand, when there are four bridging oxygen per glass-forming atom, a 3D network is obtained and Poisson's ratio is as low as  $\nu = 0.15$  (e.g., a-SiO<sub>2</sub> or a-GeO<sub>2</sub>). On the other hand, glasses with  $n_{BO} = 3$ , such as B<sub>2</sub>O<sub>3</sub>, P<sub>2</sub>O<sub>5</sub>, or As<sub>2</sub>O<sub>3</sub> glasses (P is fivefold coordinated to oxygen but with a double P = O bond leaving only three cross-linking oxygen atoms), have Poisson's ratio close to 0.3,<sup>66</sup> and glasses chiefly based on 1D structural units such as those solely made from chalcogen atoms (S, Se, and Te) possess large Poisson's ratio, typically above 0.28.<sup>6,11,14</sup> In aluminosilicate glasses, when relatively large amounts of Si are substituted by Al, such as along the 3D vertical line in Fig. 5, charge-compensating cations (Ca, Na, and Mg) are required to neutralize the charge of  $[AlO_4]^-$  tetrahedra and the atomic network disorder increases, inasmuch that higher Al coordinations show up too. Consequently,  $\nu$  increases from 0.15 for silica to 0.27 for anorthite (CaAl<sub>2</sub>-Si<sub>2</sub>O<sub>8</sub>).<sup>76</sup> Observe still along the 3D axis that the formation of CSi<sub>4</sub> tetrahedra based on fourfold covalent carbon atoms further enhances the network cross linking in comparison with a-SiO<sub>2</sub> and, consistently,  $\nu$  decreases to 0.11 for the polymer-derived SiO<sub>1.6</sub>C<sub>0.8</sub> composition.<sup>59</sup> It is noteworthy that Poisson's ratio

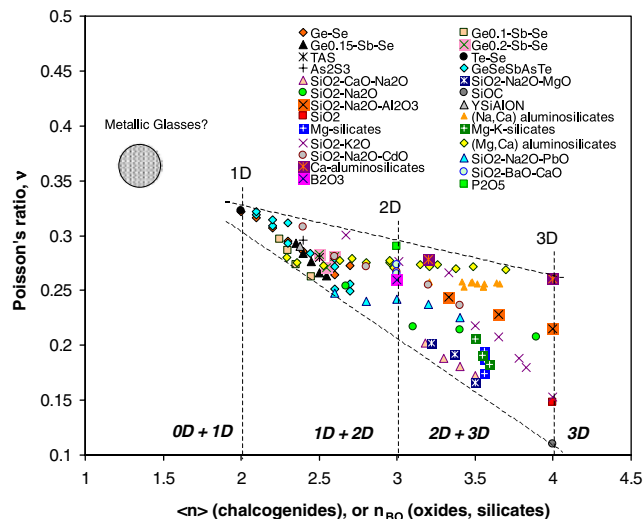
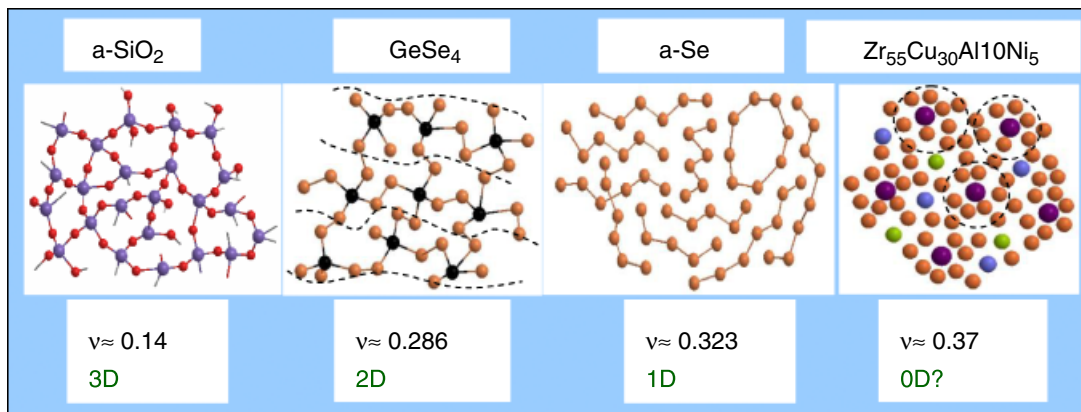


Fig. 5. Poisson's ratio as a function of the average coordination number  $\langle n \rangle$  or the number of bridging oxygen per glass-forming cation  $n_{BO}$ .



**Fig. 6.** Schematic drawings of glass atomic network structural units with increasing Poisson's ratio: a-SiO<sub>2</sub>, with each Si atoms bonded to four oxygen atoms; GeSe<sub>4</sub>, where layers of germanium (black spheres) are sandwiched between layers of selenium; a-Se that mainly consists of chain units but some rings (here Se<sub>8</sub>) may form too; and a Zr-based metallic glass possibly based on icosahedral-like clusters (Cu atoms (purple) are at the center of Zr-based icosahedra).

from 0.34 to 0.38 is predicted by extrapolating the bounds of the Poisson's ratio domain to smaller cross-link degree or to 0D structural units. Interestingly, this range is precisely the one reported for BMG,<sup>79</sup> which are known to lack structural units of a high order of symmetry. It has been recently suggested that the atomic network of such glasses consists of quasi-equivalent cluster-type units eventually packed with an icosahedral-like medium-range order<sup>117,118</sup> (Fig. 6). With a Poisson's ratio of 0.3, the glassy ice network would be based on chain-like (hydrogen-bonding chains of water molecules?) and/or cluster-like structural units (note that icosahedral water clusters were already suggested).<sup>60</sup>

#### IV. Towards Glasses Possessing High Elastic Moduli

Even though the search for glasses possessing high elastic moduli is a relatively old topic, it is of paramount interest today with the need for new light and durable materials stiffer than the presently available ones. Major issues include:

- (1) Increasing computer hard disk rotating speed;
- (2) Lowering the weight of windows (saving energy in transportation systems);
- (3) Increasing structure stiffness (buildings, biomaterials implants, and reinforcement fibers);
- (4) Optimizing ceramic-sintering additives; and
- (5) Designing glass and glass-ceramic matrices with better thermomechanical performance (aerospace industry, cooking tops, refractory seals, etc.).

For instance, in order to increase both the rotating speed and the durability of computer hard disks, Al–Mg alloys are being more and more replaced by high Young's modulus glasses. An enhancement of the elastic moduli allows also for a decrease of the weight of windows (for a given glass density) and thus for a significant decrease of the energy consumption of transportation means.<sup>146</sup>

One way to improve the volume density of energy of a glass is through cationic substitutions, looking for the optimum compromise between glass formers, possessing high bonding energies but leading to relatively low packing densities, and modifying cations, favoring a high value for  $C_g$  but introducing relatively weak bonds. Among electropositive elements, i.e., those that tend to form cations, the less-electropositive ones favor glass formation and hence do not contribute to the filling of interstitial sites and thus may be detrimental to the elastic moduli. Finally, the best results are obtained with intermediate elements such as Hf, Be, Zr, Ti, Li, and Th for which (except for Li) the electronegativity (Pauling's scale) is between 1.25–1.75.<sup>81</sup> High elastic moduli ( $E = 145$  GPa) were obtained with Mg-aluminates containing more than 25 mol% BeO (eminently toxic oxide), for the synthesis of reinforcement fibers. Aluminosilicate glasses are used when a high strength is desired: *E-* (with boron), *R-* (without boron), and *S-* (with Mg) glasses with strengths

(pristine fiber) up to 3.2–4.2 GPa are available. High elastic moduli are also obtained with the addition of rare-earth (RE) oxides ( $E = 110$ –135 GPa), the best results being obtained with the smallest RE-cations (Sc, Lu, Yb, and Y).<sup>43,46,50</sup> So far, highest moduli among oxide glasses were reported for rare-earth aluminosilicate glasses with more than 50 mol% alumina.<sup>25</sup>

A more efficient way consists in replacing some oxygen atoms by anions with higher valency, such as trivalent nitrogen or even tetravalent carbon ions. The network cross-linking degree is increased and a rigidity improvement follows. Oxynitride glasses are a good example of this approach. To the best of the knowledge of the author, the highest Young's modulus reported so far for an inorganic nonmetallic glass is  $E = 183$  GPa for  $Y_{0.146}Si_{0.232}Al_{0.034}O_{0.31}N_{0.29}$ .<sup>32</sup> Nevertheless, the substitution of oxygen for carbon in a-SiO<sub>2</sub> does not bring the expected enhancement. The reason lies in the low packing density in oxycarbide glasses. Moreover, it is not possible at standard pressure conditions to introduce more than ~15 at.% N or C atoms without avoiding crystallization in nitrogen glasses and residual free carbon in oxycarbide glasses (Fig. 7).

Indeed, in order to attain large elastic moduli, a high chemical disorder must be achieved while keeping a strong atomic frame-

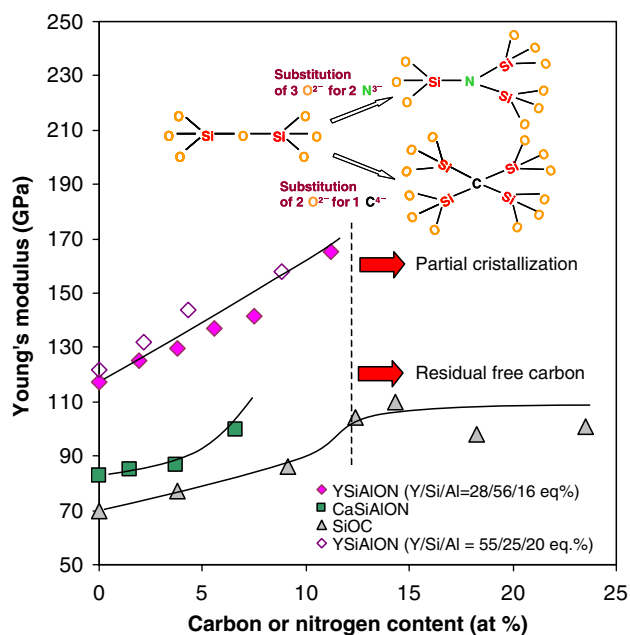


**Fig. 7.** Effect of anionic substitution on Young's modulus. Data on oxynitride glasses and oxycarbide glasses are from references [36,42,45] and [55,56,59], respectively. The insert shows the schematic of the chemical anionic substitution starting from a-SiO<sub>2</sub> as a parent glass.

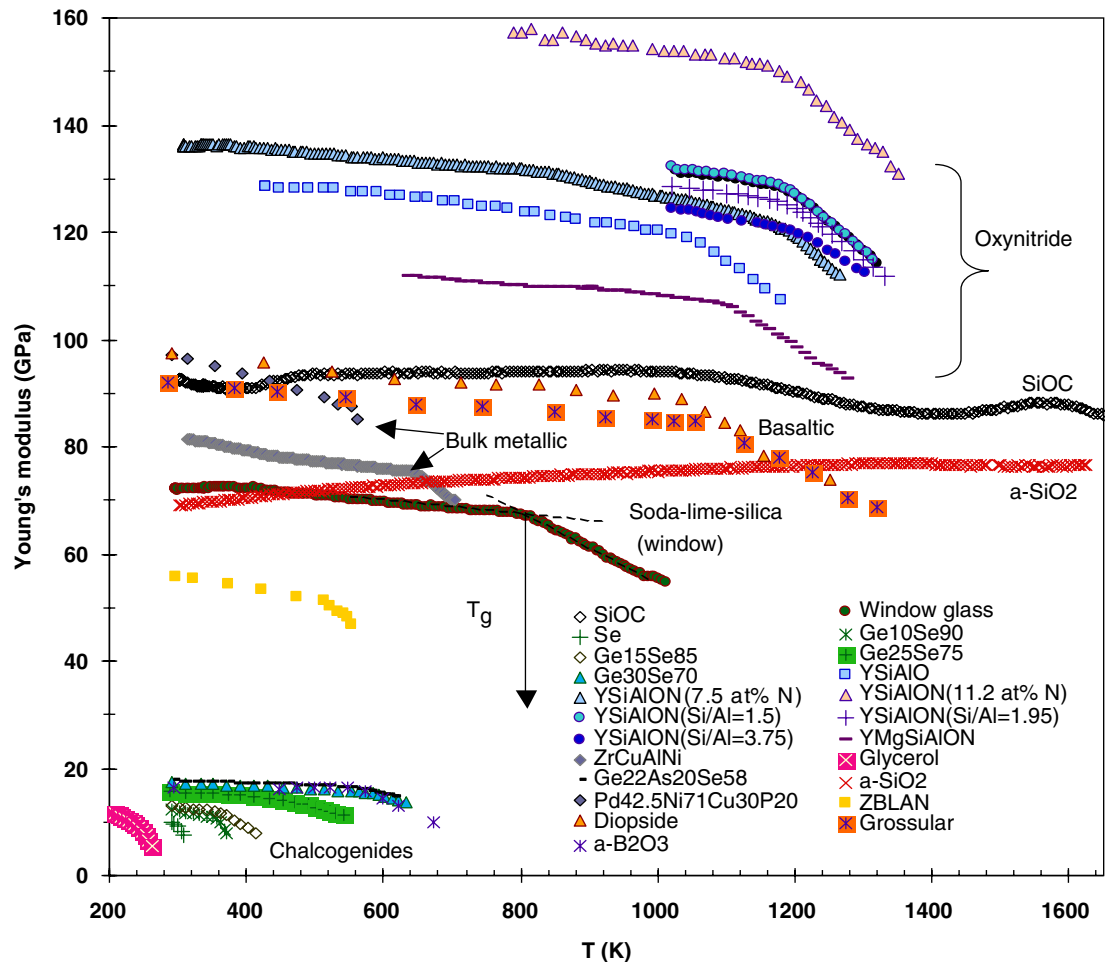


**Fig. 8.** Temperature dependence of Young's modulus. Data on chalcogenides and on the PdNiCuP glass were obtained by Gadaud and colleagues<sup>164,165</sup> and Tanaka *et al.*,<sup>189</sup> respectively, by means of mechanical vibration method. Those on a-B<sub>2</sub>O<sub>3</sub>, ZBLAN, and basaltic glasses were obtained by Youngman *et al.*,<sup>174</sup> Chen *et al.*,<sup>190</sup> and Askapour *et al.*,<sup>76</sup> respectively, by Brillouin scattering. Data on glycerol were obtained by ultrasonic echography by Slie *et al.*<sup>172</sup> Other data were obtained by the present author by means of ultrasonic echography.

work of glass-former atoms. This suggests for instance to combine modifying cations of different sizes, such as (Mg, Ca), (Ti, Zr), and (Y, Sc), with more than one glass former (Al, Si). A further improvement may be reached by adding some nitride compounds (Si<sub>3</sub>N<sub>4</sub>, AlN) to the starting oxide powders to introduce some threefold coordinated nitrogen in the glass network. In this latter case, high elastic moduli are usually observed at the expense of the loss of the glass transparency. The fact that silicon oxynitride glasses possess high elastic moduli although the Si–N bond is ~50% weaker than the Si–O one suggests that the network cross-linking degree and the atomic compactness are the major controlling factors. Hence, such as for a steel frame in mechanical design, it is the steel beams connections and the frame geometry that govern the strength and stiffness of the whole structure, rather than the individual properties of the steel beam. Besides, it turns out that nitrogen in glass results in relatively high atomic packing densities ( $C_g$  is between 0.55 and 0.63), as evidenced in Fig. 3, so that the increase of the elastic moduli might chiefly result from the increase of  $C_g$  and be only indirectly linked to the presence of nitrogen, consistently with the observation that densely packed but weakly bonded metallic atoms (in comparison with ionic-covalent bonds found in silicates) lead to remarkably stiff metallic glasses.

## V. Temperature Dependence of the Elastic Properties

### (1) Experimental Methods

It remained relatively difficult to obtain good estimations of the elastic moduli at elevated temperature in glasses until the 1950s,

with the progress in high-temperature USE, BS, and direct mechanical vibration (DMV) (including mechanical spectroscopy) measurements. The present author noticed important discrepancies between data obtained by mechanical methods before 1960 and those obtained more recently by USE, BS, or DMV on glass specimens with nominally identical composition. For example, an early report<sup>147</sup> (maybe the first one) of elasticity data in soda–lime–silica glasses above 873 K (i.e., through the  $T_g$  range) failed to reveal the transition observed near  $T_g$  in the softening regimes, which is a common feature for most glasses (see Fig. 8). In several other investigations,<sup>148,149</sup> static loading set-ups were used so that specimens significantly deformed (permanently) during the measurements. Therefore, earliest investigations,<sup>148–156</sup> such as those carried out in Jena, Germany, by Winkelmann<sup>148</sup> and Franke,<sup>152</sup> were not considered in this paragraph despite their invaluable contribution to the progress in glass science.

The velocities of mechanical waves in solids are directly correlated to the elastic moduli and to the density of the solid (see Panel A). These velocities can be estimated either by propagating acoustic waves through the solid using piezoelectric or magnetostrictive transducers for instance, or by means of the photon–phonon conversion induced by the interaction between light (a monochromatic laser beam for instance) and matter. The first case gave birth to USE techniques and the second one to BS techniques.

(A) USE: Besides the standard measurements using piezoelectric transducers and assuming infinite specimen transverse dimension,<sup>157</sup> a long beam mode set up is particularly suitable for high-temperature investigations. In this latter case,

the principle of the method<sup>158,159</sup> consists of calculating  $E$  from the velocity of an ultrasonic pulse propagating in a long, thin, and refractory wave-guide sealed to a specimen (about 1 mm × 3 mm × 40 mm). A magnetostrictive transducer (300 kHz) is used and experiments are performed under argon atmosphere with a heating rate of 5 K/min from room temperature and up to 1673 K. In the present case, the longitudinal wave velocity is about 5 km/sec, and it follows that the wavelength is about 17 mm, which is much greater than the characteristic dimension of the specimen cross section. The condition of very long wavelength, in comparison with the scale of the microstructure, is thus satisfied, and the material response is governed by the effective properties of the equivalent homogeneous medium. Furthermore, the long beam mode approximation holds, so that  $E$  can be calculated from the density ( $\rho$ ) and the longitudinal wave velocity ( $V_l$ ) according to

$$E = \rho V_l^2 \quad (7)$$

The room-temperature elastic moduli were first accurately measured by means of piezo-electric transducers (10 MHz) in direct contact with the specimen. Because the density does not vary more than a few percent over the range of these experiments, the velocity changes recorded are primarily due to the effect of temperature on the modulus of elasticity, as was already noticed by Ide.<sup>150</sup> Most data in Fig. 8 were obtained using this technique, which allow for reliable continuous *in situ* measurements with a better than  $\pm 1$  GPa.

(A) *BS*: In BS measurements<sup>76,160,161</sup> the ultrasound velocities of the longitudinal and transverse modes ( $V_{l,t}$ ) are related to the incident light wavelength ( $\lambda_o$ ) to the scattering angle ( $\phi$ ), to the refractive index of the material ( $n_r$ ), and to the frequency shift  $\Delta f_{l,t}$ , resulting from the energy conversion according to

$$V_{l,t} = \Delta f_{l,t} \lambda_o / (2n_r \sin(\phi/2)) \quad (8)$$

Elastic moduli are then derived by means of the classical equations for the linear elasticity of isotropic media (see Panel A). In most cases the scattered light is detected at 90° to the incident light ( $\phi = 90^\circ$ ). Note that with a peculiar set up consisting of two incident beams intersecting at a right angle and with the specimen being placed in the median plane (i.e., with a 45° angle between the normal to the specimen surface and the incident beams), it is possible to estimate the velocity without knowing the value for  $n_r$ .<sup>24,103</sup> High-temperature measurements are generally carried out by suspending the specimen in a small furnace with two slits at 90° one from the other allowing for the incident light beam to enter and for the scattered light to reach the collimator. Heating is mostly achieved by means of a platinum coil.

(B) *DMV*: Young's modulus can also be determined at an elevated temperature by means of mechanical vibration tech-

niques, including torsion pendulum such as in mechanical spectroscopy<sup>162</sup> and mechanical resonance frequency measurements in rectangular bars.<sup>163,164</sup> For instance, for chalcogenide glasses from the Ge–Se system and for the Ge<sub>22</sub>As<sub>20</sub>Se<sub>58</sub> glass,  $E(T)$  investigations were conducted in the bending mode with frequencies in the kHz range.<sup>164,165</sup> Experiments were conducted at 1 K/min under high vacuum ( $10^{-4}$  Pa) up to 1373 K on rectangular specimens (20 mm × 4 mm × 2 mm) maintained horizontally between steel wires located at the vibration nodes. Specimens were coated with Ag painting (thickness of the order of 4 μm) on one face in order to allow for electrostatic excitation. Furthermore, excitation and detection are insured by an electrostatic device (capacitance created between the sample and a unique electrode). Young's modulus ( $E$ ) is then given by

$$E = 0.9464 \rho F^2 L^4 / W^2 \theta(W/L, \nu) \quad (9)$$

where  $F$  is the resonance frequency,  $\rho$  the density,  $\nu$  Poisson's ratio,  $W$  and  $L$ , the beam thickness and span length, and  $\theta(W/L, \nu)$  a correcting factor close to 1.

## (2) Temperature Dependence of Young's Modulus

In all cases but a-SiO<sub>2</sub> (and to a minor extent SiOC glass), the temperature dependence of Young's modulus of glass exhibits a transition range between a slow softening rate and a faster one, corresponding to the glass transition (Fig. 8). The glass transition temperatures as well as the room temperature values of  $E$  and the softening rate immediately above  $T_g$  ( $dE/dT(T_g^+)$ ), i.e., in the supercooled liquid range, are reported in Table II.  $T_g$  temperatures as measured from  $E(T)$  curves stemming from USE are usually smaller by 10–20 K than the one obtained by dilatometry with the same heating rate. This is quite surprising since the USE method supposes fast displacements of atoms (300 kHz transducers are used) and is thus more dynamic by nature ( $T_g$  is expected to increase with the rate at which matter is moved). Further investigations are required to clarify this point. There seems to be two kinds of behavior. For relatively stiff glasses with  $E > 10$  GPa and for  $T_g \leq T \leq 1.1T_g$ ,

$$E = E(T_g) T_g / T \quad (10)$$

Less-rigid glasses such as chalcogen-rich chalcogenide glasses, glycerol, or a-B<sub>2</sub>O<sub>3</sub> exhibit a faster decrease of  $E$  with  $T$  (Fig. 9). Therefore, it seems that the temperature dependence of Young's modulus reflects the degree of "fragility" (as defined by Angell<sup>166</sup>) of the glass. In polycrystalline ceramics with glassy grain-boundary phases (see Fig. 2(c)) obtained by liquid-phase sintering, the fast softening observed beyond  $T_g$  is solely due to the effect of the liquid grain boundary films and pockets (see Rouxel *et al.*<sup>167</sup> for a review on this problem). In analogy, it is suggested that the fast softening of a glass above  $T_g$  reveals the existence of nano-domains (island organization) embedded in a softer phase.

**Table II. Estimation of the Level of Fragility of Liquids from High-Temperature Elasticity Data and Comparison with Data from Relaxation Experiments**

Glass	$T_g$ (K)	$E$ (293 K) (GPa)	$E$ ( $T_g$ ) (GPa)	$dE/dT(T_g^+)$ (MPa/K)	$\beta$ ( $\sim T_g$ ) <sup>†</sup>	$\beta^\ddagger$ (literature)
Glycerol <sup>172</sup>	186	6	9.5	−190	0.2	0.65 <sup>179</sup> or 0.435 <sup>194</sup>
Ge <sub>10</sub> Se <sub>90</sub> <sup>164</sup>	365	12.1	10	−230	0.07	0.6 <sup>195</sup>
Ge <sub>15</sub> Se <sub>85</sub> <sup>164</sup>	383	13.8	10.3	−80	0.22	0.62 <sup>195</sup>
Ge <sub>25</sub> Se <sub>75</sub> <sup>164</sup>	501	16.1	12.8	−38	0.38	0.63 <sup>195</sup>
Ge <sub>30</sub> Se <sub>70</sub> <sup>164</sup>	573	17.9	15.5	−34	0.42	0.63 <sup>195</sup>
Ge <sub>22</sub> As <sub>20</sub> Se <sub>58</sub> <sup>165</sup>	565	18	16.4	−29	0.43	0.63 <sup>195</sup>
Y <sub>12.3</sub> Si <sub>18.5</sub> Al <sub>7</sub> O <sub>54.7</sub> N <sub>7.5</sub> <sup>40</sup>	1183	150	122	−103	0.45	0.8 <sup>196</sup>
Y <sub>4.86</sub> Mg <sub>6.3</sub> Si <sub>16.2</sub> Al <sub>11.8</sub> O <sub>54.9</sub> N <sub>5.92</sub> <sup>167</sup>	1120	134	122	−105	0.52	0.75 <sup>197</sup>
Zr <sub>55</sub> Cu <sub>30</sub> Al <sub>10</sub> Ni <sub>5</sub> <sup>192</sup>	673	81.4	72.9	−108	0.65	0.7 <sup>198</sup>
Window glass <sup>193§</sup>	835	72	56	−67	0.53	0.55 <sup>179</sup> or 0.45 <sup>194</sup>
SiC <sub>0.375</sub> O <sub>1.25</sub> <sup>58</sup>	1623	110	84.8	−52	0.61	0.66 <sup>58</sup>

<sup>†</sup>Stretching exponent  $\beta$  of the KWW relationship as estimated from Eq. (11). <sup>‡</sup>Values obtained by means of relaxation experiments. <sup>§</sup>Planilux, Saint-Gobain Co.

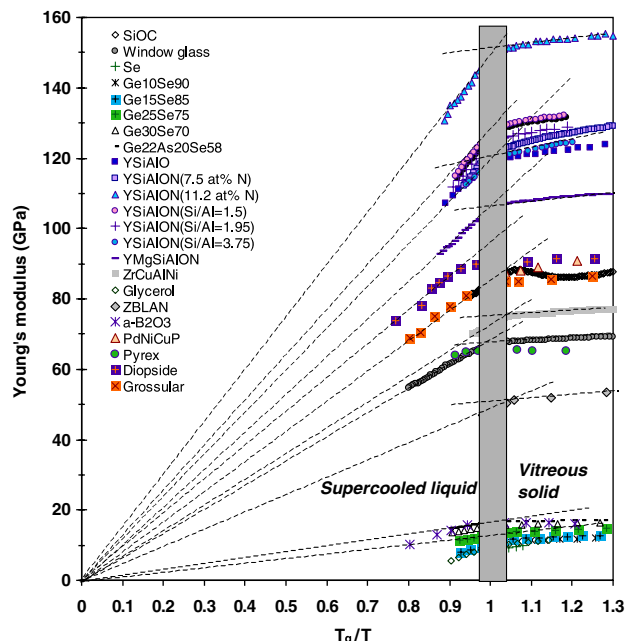


Fig. 9. Young's modulus as a function of  $T_g/T$ .

The sensitivity of the elastic moduli of glasses to temperature is thus expected to bring an original light on the possible existence of a supramolecular or mesoscopic architecture, as will be further discussed in Section V(4).

(3) Poisson's Ratio as a Probe of the Depolymerization Process Occurring Above  $T_g$

In Section V(3), Poisson's ratio appeared to be very much composition dependent and to reflect the glass network dimension-

ality. However, the glass composition does not suffice to interpret the observed correlation between  $\nu$  and the network dimensionality. Temperature comes into play. This is because elastic properties are very sensitive to temperature and  $\nu$  is expected to increase with  $T$ , as the glass gets closer to the liquid and further to the melt. The fact that glasses on the left-hand side of Fig. 5 have the lowest  $T_g$  (314 K for a-Se and about 573 K for chalcogenide glasses in general) and possess relatively large Poisson's ratio, whereas glasses on the right-hand side are the most refractory ones ( $T_g$  reaches 1623 K for silicon oxycarbide glasses), may already partly stem from different temperature intervals between  $T_g$  and ambient temperature. Sets of experimental data are reviewed in Fig. 10. In the glassy state range ( $T < T_g$ ), for all glasses but the Zr-based metallic glass,  $\nu$  increases slowly with  $T$ . The glass network structure suffers mostly from minor changes in this temperature range. There is nearly no change in a-SiO<sub>2</sub> but a small perturbation starting at  $0.8 T_g$  ( $\sim 1173$  K) and ending at  $T_g$ , which has already been observed<sup>168,169</sup> but has not been elucidated yet. The behavior of the Zr-based BMG below  $T_g$  is quite surprising and calls for further structural investigation. The decrease of  $\nu$  in the glassy state range can be tentatively interpreted on the basis of two concomitant processes, namely the structural relaxation and the progressive nucleation of dispersed crystallized domains. Annealing treatments just below  $T_g$  are known to alter the elastic moduli in an irreversible manner in such rather unstable glasses.<sup>170,171</sup> In addition, it was recently shown that in BMGs structural stabilization as well as crystallization processes may be enhanced by ultrasounds.<sup>171</sup> In Zr-based BMGs, crystallization occurs almost at  $T_g$  so that it is difficult to study the elastic properties of these materials in their liquid state. For other glasses, inspection of the high-temperature range ( $T > T_g$ ) is particularly interesting. A steep increase of  $\nu$  reveals a rapid network depolymerization, as is the case for organic chain polymers such as glycerol<sup>172</sup> or polystyrene<sup>173</sup> and also for a-B<sub>2</sub>O<sub>3</sub>,<sup>161,174</sup> In B<sub>2</sub>O<sub>3</sub> glass, the weak bonds between the planar BO<sub>3</sub> triangle

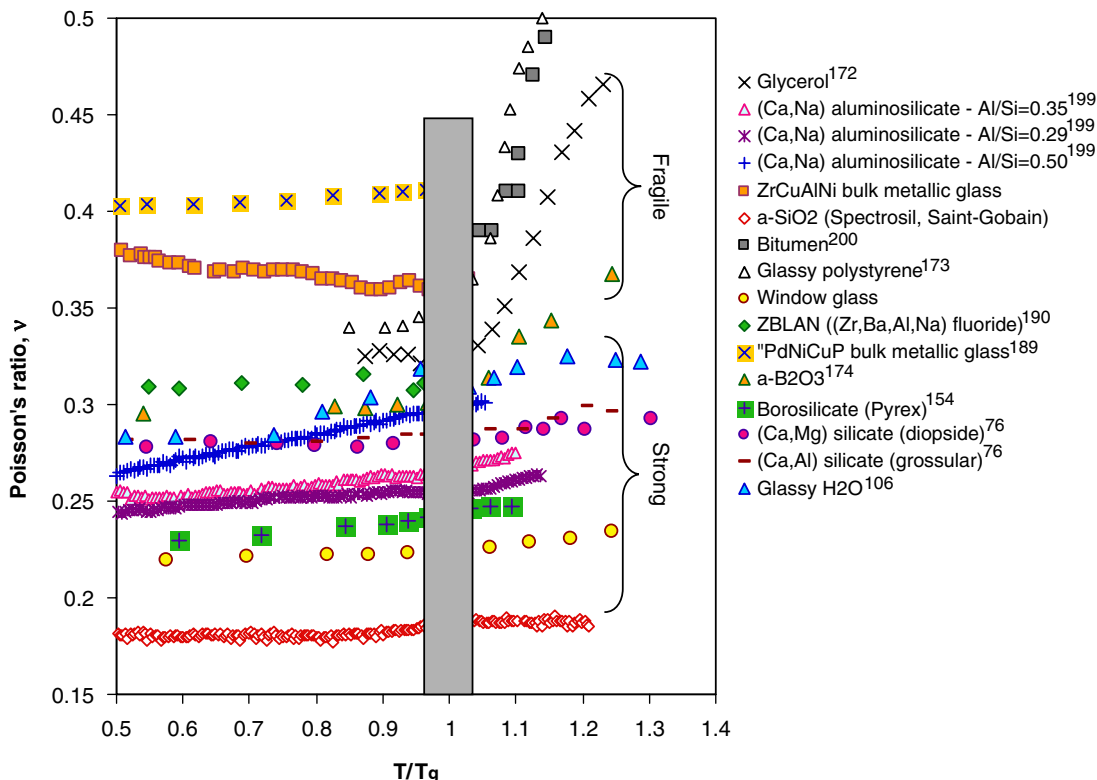
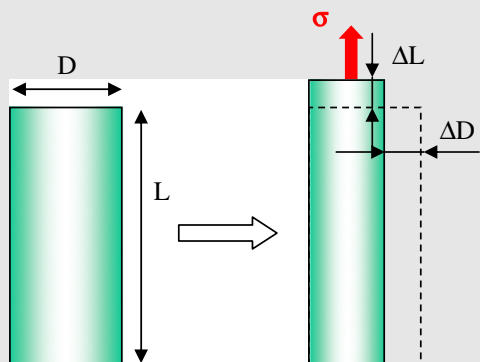


Fig. 10. Temperature dependence of Poisson's ratio for different glass systems. Data were limited to elasticity studies performed after the 1950s and using either Brillouin scattering spectroscopy or ultrasonic echography—except for the data on pyrex<sup>154</sup> obtained by a mechanical resonance technique—both for the sake of clarity and because reliable and dense sets of data can be obtained *in situ* using these techniques. Note that Hessenkemper and Brückner<sup>191</sup> reported values close to 0.5 for Poisson's ratio at  $T \sim 1.5 T_g$ , both for a borosilicate glass and a standard window glass.

## Panel B: Poisson's Ratio

Poisson's ratio ( $\nu$ )

Definition



$$\nu = -\varepsilon_t / \varepsilon_l = -L/D \Delta D / \Delta L$$

$$\Delta V/V = \text{Trace } \varepsilon = (1 - 2\nu)\sigma/E$$

Energetics considerations  $\Rightarrow -1 < \nu < 1/2$ 

Note that Poisson's ratio is strictly defined only for small strain linear elastic behavior. Most materials with low Poisson's ratio, such as amorphous silica (this is even more dramatic for auxetic materials ( $\nu < 0$ )), exhibit highly strain-dependent elastic properties

Basic relationships of linear elasticity of homogeneous media

$$E = 2(1 + \nu)\mu$$

$$K = E/[3(1 - 2\nu)]$$

where  $E$ ,  $\mu$ , and  $K$  are Young's, shear, and bulk moduli, respectively

Peculiar problems in mechanics where  $\nu$  is involved

Nanoindentation measurements:

The experimentally available elastic property is the so-called reduced modulus expressed as:  $E_r = E/(1 - \nu^2)$

Viscosity measurements using uniaxial loading tests:

The analogy between Hookean elasticity and Newtonian viscosity leads to:  $\eta_s = \sigma/[2(1 + \nu)d\varepsilon/dt]$ , where  $\eta_s$  is the shear viscosity coefficient. As viscous flow is mainly studied in a temperature range where glasses are in their liquid state ( $T > T_g$ ) so that they deform with little volume change,  $\nu$  is often assumed to be 0.5 so that the former expression reduces to  $\eta_s = \sigma/(3d\varepsilon/dt)$

Hydrostatic stress along a vertical axis under a sharp contact loading (load  $P$ )

$\sigma_h = -(1 + \nu)P/(3\pi r^2)$ , where  $r$  is the distance from the surface (from Boussinesq's elasticity solution)

It is noteworthy that there are numerous problems where  $\nu$  comes into play in the form of  $1/(1 - \nu^2)$  so that solutions are very sensitive to Poisson's ratio especially for low  $\nu$  values

units (to be compared with the 3D cross-linked network found in  $B_2O_3$  crystal) lead to a temperature-dependent structure, with a rapid desintegration starting abruptly right at  $T_g$ . Indeed, it was found by Hassan *et al.*<sup>175</sup> that the fraction of boroxol rings consisting of three corner-sharing  $BO_3$  units decreases dramatically with temperatures above  $T_g$  (by 2/3 from 400 to 1200 K), through the conversion to chains of  $BO_3$  triangles. Hence, the connectivity of the liquid is strongly reduced whereas triangular molecular units still survive up to rather high temperatures above  $T_g$ . Addition of  $SiO_2$  greatly enhanced the 3D polymerization and its thermal stability as illustrated by the data obtained on a borosilicate glass<sup>154</sup> (pyrex type, Si/B = 3.5). In the case of aluminosilicate glasses, the general tendency is that a high number of nonbridging oxygen per tetrahedron results in a rapid increase of  $\nu$  with  $T$ . High alkaline or alkaline-earth contents favor sheet-like units (Al tetrahedra with  $n_{BO} = 3$ ) and results in a low network connectivity as shown by Neuville *et al.*<sup>139</sup> and in a higher temperature sensitivity, whereas at high (Al, Si) contents the network consists mainly of fourfold coordinated (Al, Si) and is well polymerized. However, the role of aluminum is far from being simple. Although basaltic-like compositions exhibit considerable Al/Si disorder with Al-O-Al links (instead of the Al-O-Si ordering found in crystalline counterparts) and a significant amount of nonbridging oxygen atoms (whereas four bridging oxygen per tetrahedron are predicted from the stoichiometry),<sup>136-138</sup> they show little change in  $\nu$  with  $T$ , even above  $T_g$  up to 1.3  $T_g$ . It is noteworthy that for aluminosilicate glasses in which the amounts of alkaline and alkaline-earth are sufficient to compensate the negative charge within Al tetrahedra (series with different Al/Si ratios in Fig. 10), a monotonic increase of  $\nu$  is observed from 0.5 to 1.1  $T_g$  and in the case of the

composition with Al/Si = 0.5 (58.3%  $SiO_2$ , 14.7%  $Al_2O_3$ , 25.6% CaO, and 1.4  $Fe_2O_3$ ) there is even no change in the slope at  $T_g$  but a continuous increase of  $\nu$  through the glass transition. This suggests that some structural reorganization (fourfold to (five, six)-fold coordination change of Al?) starts well below  $T_g$  in aluminosilicate glasses independent of the state of the material (glassy or liquid). (Panel B).

The cases of a- $SiO_2$  and glassy water are particularly interesting because these glasses are often considered as good examples of polymorphism and exhibit unusual behaviors. In glassy water,<sup>106</sup> the glass experiences transitions from the high-density amorphous phase to the low-density amorphous phase between 100 and 147 K and to cubic and hexagonal ice at higher temperature. The structural transformation between the two kinds of amorphous ice is accompanied by a significant increase of  $\nu$ , from  $\sim 0.285$  to  $\sim 0.31$ . Crystallization above 147 K induces another jump of  $\nu$  from  $\sim 0.31$  to 0.33. These jumps stem from the fact that the shear modulus decreases faster than Young's modulus when  $T$  increases. Although such an increase is expected through the glass/liquid transition, it is far from being common in the case of the glass/crystal phase transformation. Owing to our analysis of the  $\nu$  versus average coordination (Section III(3)), this would mean that the cross-link degree (or the dimensionality) is greater in the glass than in the crystallized phases of water, and in the low-density amorphous phase than in the high-density one as well. In a- $SiO_2$ , an amorphous-amorphous transformation was also suggested by Huang and Kieffer<sup>176</sup> to explain the well-documented thermomechanical anomalies (for instance the increase of  $E$  with  $T$ ).<sup>176,177</sup> This transformation appears more gradual in a- $SiO_2$  than in glassy water and would consist in atomic displacements similar to those associated with

the  $\alpha$ - to  $\beta$ -cristoballite phase transformation in crystalline silica.<sup>177</sup> The  $\beta$ -form is stiffer than the  $\alpha$  one, the natural temperature weakening of the interatomic bonding is compensated. As a consequence, almost no change but a slight increase of  $E$  is observed with increasing temperature (Fig. 8). The fact that  $\nu$  remains almost constant from 0.5 to 1.2  $T_g$  further suggests that the liquid keeps a strong memory of the atomic structure of the glassy solid, with little changes of the average coordination and dimensionality throughout the glass transition range.

#### (4) High-Temperature Elasticity and the Fragility of Glass-Forming Liquids

The temperature sensitivity of the elastic moduli in the liquid range depends much on the glass composition (see Section V(2)). The rate at which the glass network structure degrades above  $T_g$  was already viewed by Masnik *et al.*<sup>178</sup> and Youngman *et al.*<sup>174</sup> as indicative of the fragility of the liquid. Indeed, the softening rate immediately above  $T_g$  can be used to evaluate the fragility of the liquid from the correlation existing between the softening rate and the relaxation kinetics. Relaxation phenomena in glasses mostly follow a stretch exponential function (also referred to as the KWW relationship),  $\phi(t) = \exp[-(t/\tau)^\beta]$ . It was shown in a previous work<sup>167</sup> that  $\beta$  can be roughly estimated from the following expression

$$\beta = \frac{1}{1 - (T/E)(\partial E/\partial T)} \quad (11)$$

The value for  $\beta$  is between 0 and 1, and reflects the degree of cooperativity of the relaxation process:  $\beta$  is inversely proportional to the width of the relaxation time spectrum. A frozen state corresponds to a small value whereas a value of 1 is associated with a classical Debye relaxation. Perfectly disordered—or ideal—liquids exhibit  $\beta$  values close to 1. It was suggested that the so-called “strong” glasses such as a-SiO<sub>2</sub>, for which viscosity decreases slowly with  $T$  for  $T_g \leq T \leq 1.1T_g$ , have much higher  $\beta$  values in comparison with fragile glasses, such as glycerol and chalcogen-rich glasses.<sup>179</sup> Brawer<sup>180</sup> showed that for most highly cross-linked glasses  $\beta$  approaches 0.5–0.6, contrary to polymeric liquids or weakly coordinated chalcogenide glasses for which  $\beta$  is smaller. For instance, oxynitride glasses exhibit  $\beta$ -values ranging from 0.45 to 0.52. It is noteworthy that replacing  $E(T)$  by its expression for the strongest glasses (Eq. (10)) gives  $\beta = 0.5$  in Eq. (11). For glasses based on chain-like structural units,  $\beta$  is much lower: 0.07 for GeSe<sub>9</sub> and 0.2 for Glycerol (Table II).

Owing to the strong sensitivity of  $\nu$  to temperatures above  $T_g$  and to the large differences observed between the experimental  $\nu(T)$  data collected within various glass systems, attempts to correlate ambient values for  $\nu$  to physical properties measured above  $T_g$  are debatable, especially when  $\nu$  values rank differently at  $T_g$  and at room temperature as demonstrated by the fact that several experimental curves cross each other in Fig. 10. The correlation proposed recently by Novikov and Sokolov<sup>181</sup> between the fragility ( $m$ ) of glass-forming liquid ( $m = \partial \log_{10} \eta / \partial (T_g/T)$  at  $T = T_g$ , where  $\eta$  is the apparent shear viscosity) and the room temperature Poisson’s ratio ( $m$  increases with  $\nu$ ) is therefore questionable, as was later demonstrated by Yannopoulos and Johari<sup>182</sup> considering a much broader range of glass compositions with different bond types, from which no clear correlation could be arrived at. Because the network connectivity and its dependence on temperature are expected to affect  $\nu$  and  $\eta$  the same way, we suggest future investigators to pay more attention to  $\nu(T)$ .

## VI. Other Elasticity Issues in Glasses

### (1) Effects of Annealing Treatments

Annealing treatments reduce the free volume content and increase the atomic packing density. Consequently, they induce a

slight increase of the elastic moduli. For instance, Gillod<sup>153</sup> observed a 15% increase of  $E$  in a borosilicate glass ( $\sim 22\%$  B<sub>2</sub>O<sub>3</sub>) after annealing of a quenched sample. A larger increase was reported by Concustell *et al.*<sup>183</sup> in a Cu<sub>60</sub>Zr<sub>22</sub>Ti<sub>18</sub> bulk metallic alloy after annealing at  $T_g$ . In this latter case  $E$  increased from 106 (as-quenched) to 115 GPa after reheating to  $T_g$  to improve the structural relaxation and cooling (i.e., a 8.5% increase). A further improvement, up to 142 GPa, was observed after a 120-min long plateau at  $T_g$  as a result of primary crystallization.

### (2) Pressure Dependence of the Elastic Moduli

In comparison with the number of data dealing with high-temperature elasticity, only few high-pressure ( $P$ ) studies were reported.<sup>3,184,185</sup> Nevertheless, elasticity investigations under high pressure also reveal interesting structural changes regarding either the coordination number or the atomic packing density. Using thermodynamics data and high-temperature elasticity results, Kurkjian *et al.*<sup>184</sup> predicted that tetrahedral glasses such as SiO<sub>2</sub>, BeF<sub>2</sub>, and GeO<sub>2</sub> all exhibit a negative pressure dependence of their shear moduli and found a direct correlation with Poisson’s ratio: the smaller the  $\nu$ , the more negative the pressure dependence becomes. The pressure dependence is expected to become positive for  $\nu > 0.25$  (B<sub>2</sub>O<sub>3</sub>, with  $\nu = 0.26$ , would exhibit a positive dependence). It is found experimentally that for silica, the elastic moduli first decrease with  $P$ , up to  $P \sim 2.5$  GPa.<sup>186</sup> At higher pressure the elastic moduli increase as is the case for most materials. In silica and silicate glasses, and in low Poisson’s ratio glasses in general,<sup>187</sup> high pressure induces permanent densification. Above 20 GPa, the density of a-SiO<sub>2</sub> approaches the one of quartz. In silica-based glasses, very high pressures are found to increase the average coordination of silicon as well as the atomic packing density. This results in a gradual increase of  $\nu$  with  $P$ , from 0.15 to  $\sim 0.3$  above 20 GPa.<sup>185</sup> In the case of glassy water,  $K$  increases but  $\mu$  decreases with increasing pressure.<sup>106</sup>

## VII. Conclusion and Perspectives

Elastic moduli are relatively easily measurable macroscopic parameters. It is shown in this study that they can be used to probe the glass network architecture, at the nano-, micro-, and mesoscopic scales. Comparative investigations conducted on series of glasses from different glass systems, with metallic, ionic, or covalent bonding, reveal the following tendencies:

(1) There is no direct relationship between elastic moduli and  $T_g$ .

(2) Poisson’s ratio ( $\nu$ ) correlates with the atomic packing density ( $C_g$ ) and with the glass network dimensionality. The atomic packing density  $C_g$  increases with  $\nu$ . Poisson’s ratio  $\nu$  ranges from  $\sim 0.1$  for a SiOC glass characterized by a large fraction of free volume, to  $\sim 0.4$  for Pd- and Zr-based BMG. The network dimensionality (chains, layers, etc.) increases monotonically with the mean coordination number or with the fraction of bridging oxygen atoms per tetrahedron, but changes inversely with  $\nu$ . Hence, for chalcogenide glasses, the network of which resembling the one of chain-polymers,  $\nu > 0.25$ , whereas in the case of 3D organization, such as in SiO<sub>2</sub>-rich glasses,  $\nu < 0.2$ .

(3) High elastic moduli are favored by structural disorder and in the search for stiff glasses, atomic packing density seems to predominate over bond strength. This implies both chemical diversity and large coordination numbers for the cations added to the main glass-forming species. Anionic diversity and for instance addition of anions of valency larger than the one of oxygen also contributes to the stiffening. Multicomponent oxynitride glasses provide a good example of this approach.

(4) The temperature dependence of the elastic properties above  $T_g$  can be discussed in the light of the “fragile” versus “strong” character of the liquid. The temperature sensitivity of  $\nu$  in the liquid range can be viewed as a consequence of the depolymerization occurring above  $T_g$ , the rate of which being suggested as indicative of the glass-forming liquid fragility.  $\nu$

depends much on temperature above  $T_g$  but stays mostly lower than 0.5 up to  $T = 1.3 T_g$  except for weakly cross-linked materials such as chain polymers.

At the atomic scale, the understanding of the elastic properties of glasses will undoubtedly benefit from improved structural simulations based on *ab initio* and molecular dynamics (MD) calculations. However, better-refined molecular orbital descriptions are needed to account for the subtle atomic organization in multicomponent glasses. At the opposite length scale of mechanical design and civil engineering, the feasibility for making glasses with specific elastic properties opens new realms of possibilities, for the fabrication of high precision tools (surgery equipments made from BMG) for hard disk drives rotating at very high speeds (over 10000 rpm) or even in the building industry for innovative load bearing glass structures. In this latter case, large glass beams and plates are required, and strength calculations as well as safety criteria in service required a good control over the elastic properties.

### Acknowledgments

This article is based on experimental results obtained by the author through fruitful collaborations with R. Riedel (TU Darmstadt, Germany), G.-D. Soraru (University of Trento, Ireland), S. Hampshire (University of Limerick, Ireland), Y. Kawamura (University of Kumamoto, Japan), Y. Yokoyama (University of Tohoku, Japan), C. Gault and M. Huger (ENSCI, Limoges, France), P. Gadaud (ENSM, Poitiers, France), F. Augereau (LAIN, Montpellier, France), and the "Glass and Ceramics Laboratory" (University of Rennes 1, France). V. Keryvin, J.-P. Guin, J.-C. Sangleboeuf, B. Truffin, R. Dauce, and H. Ji (LARMAUR, University of Rennes 1, France) are also gratefully acknowledged for their support and for their experimental assistance (measurements on BMG and a-SiO<sub>2</sub>).

### References

- 1H. J. McSkimin and E. S. Fisher, "Measurement of Ultrasonic Wave Velocities for Solids," *J. Appl. Phys.*, **31**, 627 (1960). See also *ibid.*: *J. Acoust. Soc. Am.*, **33** 12 (1961).
- 2J. A. Savage and S. Nielsen, "Preparation of Glasses Transmitting in the Infra-red between 8 and 15 Microns," *Phys. Chem. Glasses*, **5** [3] 82–6 (1964).
- 3J. C. Thompson and K. E. Bayley, "A Survey of the Elastic Properties of Some Semiconducting Glasses under Pressure," *J. Non-Cryst. Sol.*, **27**, 161–72 (1978).
- 4J. C. Phillips, "Topology of Covalent Non-Crystalline Solids I: Short-Range Order in Chalcogenide Alloys," *J. Non-Cryst. Sol.*, **34**, 153–81 (1979).
- 5M. F. Thorpe, "Continuous Deformation in Random Networks," *J. Non-Cryst. Sol.*, **57**, 355–70 (1983).
- 6S. Mahadevan, A. Giridhar, and A. K. Singh, "Elastic Properties of Ge–Sb–Se Glasses," *J. Non-Cryst. Sol.*, **57**, 423–30 (1983).
- 7M. Poulain, "Halide Glasses," *J. Non-Cryst. Sol.*, **56** [1–3] 1–14 (1983).
- 8K. Tanaka, "Structural Phase Transitions in Chalcogenide Glasses," *Phys. Rev. B*, **39**, 1270–9 (1989).
- 9J. Portier, "Halogenide, Chalcogenide and Chalcogenide Glasses: Materials, Models, Applications," *J. Non-Cryst. Sol.*, **112** [1–3] 15–22 (1989).
- 10J. Lucas, "Halide Glasses," in *Glasses and Amorphous Materials*, Edited by J. Zarzycki. VCH, New York, 1991, pp. 457–488.
- 11A. N. Sreeram, A. K. Varshneya, and D. R. Swiler, "Molar Volume and Elastic Properties of Multicomponent Chalcogenide Glasses," *J. Non-Cryst. Sol.*, **128**, 294–309 (1991).
- 12A. K. Varshneya, *Fundamentals of Inorganic Glasses*. Academic Press Inc., Boston, 1994, pp. 7.
- 13V. Q. Nguyen, J. S. Sanghera, I. D. Aggarwal, and I. K. Lloyd, "Physical Properties of Chalcogenide and Chalcogenide Glasses," *J. Am. Ceram. Soc.*, **83** [4] 855–9 (2000).
- 14J. P. Guin, T. Rouxel, J. C. Sangleboeuf, I. Melscoët, and J. Lucas, "Hardness, Toughness, and Scratchability of Germanium–Selenium Chalcogenide Glasses," *J. Am. Ceram. Soc.*, **85** [6] 1545–52 (2002).
- 15A. Delben, Y. Messaddeq, M. D. Caridade, and M. E. Aegerter, "Mechanical Properties of ZBLAN Glasses," *J. Non-Cryst. Sol.*, **161**, 165–8 (1993).
- 16M. Poulain, M. Poulain, and J. Lucas, "History of Fluorinated Glasses," *Actualité Chimique*, **117–118** (Suppl.) 301–2 (2006).
- 17A. Peker and W. L. Johnson, "A Highly Processable Metallic Glass: Zr<sub>41.2</sub>Ti<sub>13.8</sub>Cu<sub>12.5</sub>Ni<sub>10.6</sub>Be<sub>22.5</sub>," *Appl. Phys. Lett.*, **63** [17] 2342–4 (1993).
- 18A. Inoue, T. Zhang, and T. Masumoto, "Glass-Forming Ability of Alloys," *J. Non-Cryst. Sol.*, **156–158** [2] 473–80 (1993).
- 19J. Philibert, A. Vignes, Y. Bréchet, and P. Combrade, *Métallurgie: du minéral au matériau*. Pub. Masson, Paris, 1998.
- 20A. Inoue, *Bulk Amorphous Alloys, Practical Characteristics and Applications*. Trans Tech Publications Inc., Zurich, 1999.
- 21M. Ohtsuki, R. Tamura, S. Yoda, and T. Ohmura, "Hard Metallic Glass of Tungsten-Based Alloy," *Appl. Phys. Lett.*, **84**, 4911 (2004).
- 22W. H. Wang, "Elastic Moduli and Behaviors of Metallic Glasses," *J. Non-Cryst. Sol.*, **351**, 1481–5 (2005).

- 23S. Tanabe, K. Hirao, and N. Soga, "Elastic Properties and Molar Volume of Rare-Earth Aluminosilicate Glasses," *J. Am. Ceram. Soc.*, **75** [3] 503–6 (1992).
- 24A. Yeganeh-Haeri, C. T. Ho, R. Weber, J. Diefenbacher, and P. F. McMillan, "Elastic Properties of Aluminate Glasses via Brillouin Spectroscopy," *J. Non-Cryst. Sol.*, **241**, 200–3 (1998).
- 25J. Johnson, R. Weber, and M. Grimsditch, "Thermal and Mechanical Properties of Rare Earth Aluminate and Low-Silica Aluminosilicate Optical Glasses," *J. Non-Cryst. Sol.*, **351**, 650–5 (2005).
- 26S. Inaba, K. Fujino et, and S. Morinaga, "Young's Modulus and Compositional Parameters of Oxide Glasses," *J. Am. Ceram. Soc.*, **82** [12] 3501–7 (1999).
- 27J. A. Sampaio, M. L. Baesso, S. Gama, A. A. Coelho, J. A. Eiras, and I. A. Santos, "Rare Earth Doping Effect on the Elastic Moduli of Low Silica Calcium Aluminate Glasses," *J. Non-Cryst. Sol.*, **304**, 293–8 (2002).
- 28X. Zou and H. Toratami, "Compositional Design of High Modulus Glasses for Disk Substrates," *J. Non-Cryst. Sol.*, **290**, 180–8 (2001).
- 29L. G. Hwa, T. H. Lee, and S. P. Szu, "Elastic Properties of Lanthanum Aluminosilicate Glasses," *Mat. Res. Bull.*, **39**, 33–40 (2004).
- 30A. Makishima, Y. Tamura, and T. Sakaino, "Elastic Moduli and Refractive Indices of Aluminosilicate Glasses Containing Y<sub>2</sub>O<sub>3</sub>, La<sub>2</sub>O<sub>3</sub> and TiO<sub>2</sub>," *J. Am. Ceram. Soc.*, **61** [5–6] 247–9 (1978).
- 31N. Hémono, J. Rocherullé, M. Le Floch, B. Bureau, and P. Bénard-Rocherullé, "Synthesis, Characterization and Devitrification Behaviour of an Yttrium Containing Boroaluminate Glass," *J. Mater. Sci.*, **41** [2] 445–53 (2006).
- 32D. R. Messier and A. Broz, "Microhardness and Elastic Moduli of Si–Y–Al–O–N Glasses," *Comm. Am. Ceram. Soc.*, **65** [8] C-123 (1982).
- 33R. E. Loehman, "Preparation and Properties of Oxynitride Glasses," *J. Non-Cryst. Solids*, **56**, 123–34 (1983).
- 34S. Sakka, K. Kamiya, and T. Yoko, "Preparation of Ca–Al–Si–O–N Oxynitride Glasses," *J. Non-Cryst. Sol.*, **56**, 147–52 (1983).
- 35S. Hampshire, R. A. L. Drew, and K. H. Jack, "Viscosities, Glass Transition Temperatures, and Microhardness of Y–Si–Al–O–N Glasses," *J. Am. Ceram. Soc.*, **3**, C46–7 (1984).
- 36C. Ecolivet and P. Verdier, "Propriétés élastiques et indices de réfraction de verres azotes," *Mater. Res. Bull.*, **19**, 227–31 (1984).
- 37D. R. Messier, "Preparation and Properties of Y–Si–Al–O–N Glasses," *Int. J. High Technol. Ceram.*, **3**, 33–41 (1987).
- 38J. Rocherullé, C. Ecolivet, M. Poulain, P. Verdier et, and Y. Laurent, "Elastic Moduli of Oxynitride Glasses: Extension of Makishima and Mackenzie's Theory," *J. Non-Cryst. Sol.*, **108**, 187–93 (1989).
- 39S. Sakka, *Oxynitride Glasses*. Uchida Rokakuho Pub. Co. Ltd, Tokyo, Japan, 1989 (in Japanese).
- 40T. Rouxel, M. Huger, and J. L. Besson, "Rheological Properties of YSiAlON Glasses- Elastic Moduli, Viscosity and Creep," *J. Mater. Sci.*, **27**, 279–84 (1992).
- 41A. Sekkat, S. Etienne, C. Maï, J. Perez, C. Garnier, P. Verdier, and Y. Laurent, "Effect of Nitrogen Content on the Physical and Mechanical Properties of Oxynitride Glasses," *Supp J. Phys. III*, **2**, C2 253–6 (1992).
- 42S. Hampshire, E. Nestor, R. Flynn, J. L. Besson, T. Rouxel, H. Lemercier, P. Goursat, M. Sebai, D. P. Thompson, and K. Liddell, "Yttrium Oxynitride Glasses: Properties and Potential for Crystallisation to Glass–Ceramics," *J. Eur. Ceram. Soc.*, **14**, 261–73 (1994).
- 43M. Ohashi, K. Nakamura, K. Hirao, S. Kanzaki, and S. Hampshire, "Formation and Properties of Ln–Si–O–N Glasses (Ln = Lanthanides or Y)," *J. Am. Ceram. Soc.*, **78** [1] 71–6 (1995).
- 44H. Lemercier, T. Rouxel, D. Fargeot, J. L. Besson, and B. Piriou, "Yttrium Oxynitride Glasses: Structure and Mechanical Properties—Elasticity and Viscosity," *J. Non-Cryst. Sol.*, **201**, 128–45 (1996).
- 45E. Y. Sun, P. F. Becher, S. L. Hwang, S. B. Waters, G. M. Pharr, and T. Y. Tsui, "Properties of Silicon–Aluminum–Yttrium Oxynitride Glasses," *J. Non-Cryst. Sol.*, **208**, 162–9 (1996).
- 46Y. Menke, V. Peltier-Baron, and S. Hampshire, "Effect of Rare-Earth Cations on Properties of Sialon Glasses," *J. Non-Cryst. Sol.*, **276**, 145–50 (2000).
- 47R. Dauce, P. Verdier, Y. Laurent, and J. A. Odriozola, "An Approach to the Chemistry of Fracture in Oxynitride Glasses," *Ann. Chim. Sci. Mat.*, **28**, 79–86 (2003).
- 48M. J. Pomeroy, C. Mulcahy, and S. Hampshire, "Independent Effects of Nitrogen Substitution for Oxygen and Yttrium Substitution for Magnesium on the Properties of Mg–Y–Si–Al–O–N Glasses," *J. Am. Ceram. Soc.*, **86** [3] 458–64 (2003).
- 49P. F. Becher, M. J. Lance, M. K. Ferber, M. J. Hoffman, and R. L. Satet, "The Influence of Mg Substitution for Al on the Properties of SiMeRE Oxynitride Glasses," *J. Non-Cryst. Sol.*, **333**, 124–8 (2004).
- 50F. Lofaj, T. Rouxel, and M. Hoffmann, "Thermal, Elastic and Dielectric Properties of the Rare-Earth Containing Oxynitride Glasses," *Silicates Ind.*, **69** [5–6] 95–104 (2004).
- 51F. Lofaj, R. Satet, M. J. Hoffmann, and A. R. de Arellano Lopez, "Thermal Expansion and Glass Transition Temperature of the Rare-Earth Doped Oxynitride Glasses," *J. Eur. Ceram. Soc.*, **24**, 3377–85 (2004).
- 52P. F. Becher, M. J. Lance, M. K. Ferber, M. J. Hoffman, and R. L. Satet, "The Influence of Mg Substitution for Al on the Properties of SiMeRe Oxynitride Glasses," *J. Non-Cryst. Sol.*, **333**, 124–8 (2004).
- 53F. Lofaj, S. Dériano, M. LeFloch, T. Rouxel, and M. J. Hoffmann, "Structure and Rheological Properties of the RE–Si–Mg–O–N Glasses," *J. Non-Cryst. Sol.*, **344**, 8–16 (2004).
- 54J. Homeny, S.H. Nelson et, and G. G. Risbud, "Oxycarbide Glasses in the Mg–Al–Si–O–C System," *J. Am. Ceram. Soc.*, **71** [5] 386–90 (1988).
- 55G. M. Renlund, S. Prochazka, and R. H. Doremus, "Silicon Oxycarbide Glasses: Part II. Structure and Properties," *J. Mater. Res.*, **6** [12] 2723–34 (1991).

- <sup>56</sup>G. D. Soraru, E. Dallapiccola, and G. D'Andrea, "Mechanical Characterization of Sol-Gel-Derived Silicon Oxycarbide Glasses," *J. Am. Ceram. Soc.*, **79** [8] 2074–80 (1996).
- <sup>57</sup>T. Rouxel, G. Massouras, and G-D. Soraru, "High Temperature Behavior of a Gel-Derived SiOC Glass: Elasticity and Viscosity," *J. Sol-Gel Sci. Technol.*, **14**, 87–94 (1999).
- <sup>58</sup>T. Rouxel, G. D. Soraru, and J. Vicens, "Creep Viscosity and Stress Relaxation of Gel-Derived Silicon Oxycarbide Glasses," *J. Am. Ceram. Soc.*, **84** [5] 1052–8 (2001).
- <sup>59</sup>C. Moysan, R. Riedel, R. Harshe, T. Rouxel, and F. Augereau, "Mechanical Characterization of a Polysiloxane-Derived SiOC Glass," *J. Eur. Ceram. Soc.*, **27**, 397–403 (2007).
- <sup>60</sup>P. G. Debenedetti, "Supercooled and Glassy Water," *J. Phys. Cond. Mater.*, **15**, R1669–726 (2003).
- <sup>61</sup>V. Rajendran, N. Palanivelu, B. K. Chaudhuri, and K. Goswami, "Temperature and Composition Dependence of the Elastic Properties of Semiconducting (100-x)V<sub>2</sub>O<sub>5</sub>-xPbO Oxide Glasses," *Phys. Stat. Sol. (a)*, **191** [2] 445–57 (2002).
- <sup>62</sup>K. Suzuya, D. L. Price, C. K. Loong, and S. Martin, "Structure of Vitreous P<sub>2</sub>O<sub>5</sub> and Alkali Phosphate Glasses," *J. Non-Cryst. Sol.*, **232–234**, 650–7 (1998).
- <sup>63</sup>K. H. Chang, T. H. Lee, and L. G. Hwa, "Structure and Elastic Properties of Iron Phosphate Glasses," *Chin. J. Phys.*, **41** [4] 414–21 (2003).
- <sup>64</sup>J. H. Campbell and T. I. Suratwala, "Nd-Doped Phosphate Glasses for High-Energy/High-Peak-Power Lasers," *J. Non-Cryst. Sol.*, **263–264**, 318–41 (2000).
- <sup>65</sup>V. Rajendran, A. N. Begum, M. A. Azooz, and F. H. El Batal, "Microstructural Dependence on Relevant Physical-Mechanical Properties on SiO<sub>2</sub>-Na<sub>2</sub>O-CaO-P<sub>2</sub>O<sub>5</sub> Biological Glasses," *Biomaterials*, **23**, 4263–75 (2002).
- <sup>66</sup>B. Bridge, N. D. Patel, and D. N. Waters, "On the Elastic Constants and Structure of the Pure Inorganic Oxide Glasses," *Phys. Stat. Sol. (a)*, **77**, 655–68 (1983).
- <sup>67</sup>J. M. Jewell, P. L. Higby, and I. D. Aggarwal, "Properties of BaO-R<sub>2</sub>O<sub>3</sub>-Ga<sub>2</sub>O<sub>3</sub>-GeO<sub>2</sub> (R = Y, Al, La, and Gd) Glasses," *J. Am. Ceram. Soc.*, **77** [3] 697–700 (1994).
- <sup>68</sup>S. S. Baya, G. D. Chin, J. S. Sanghera, and I. D. Aggarwal, "Germanate Glass as a Window for High Energy Laser Systems," *Optics Express*, **14** [24] 11687–93 (2006).
- <sup>69</sup>L. G. Hwa and W. C. Chao, "Velocity of Sound and Elastic Properties of Lanthanum Gallo-Germanate Glasses," *Mater. Chem. Phys.*, **94**, 37–41 (2005).
- <sup>70</sup>A. Makishima and J. D. Mackenzie, "Direct Calculation of Young's Modulus of Glass," *J. Non-Cryst. Sol.*, **12**, 35–45 (1973).
- <sup>71</sup>I. Z. Hager, "Elastic Moduli of Boron Oxyluoride Glasses: Experimental Determinations and Application of Makishima and Mackenzie's Theory," *J. Mater. Sci.*, **37**, 1309–13 (2002).
- <sup>72</sup>M. Kodama, "Ultrasonic Velocity in Caesium Borate Glasses," *J. Mater. Sci. Lett.*, **11**, 1406–7 (1992).
- <sup>73</sup>J. Shroeder, R. Mohr, P. B. Macedo, and C. J. Montrose, "Rayleigh and Brillouin Scattering in K<sub>2</sub>O-SiO<sub>2</sub> Glasses," *J. Am. Ceram. Soc.*, **56** [10] 510–4 (1973).
- <sup>74</sup>S. Deriano, T. Rouxel, M. LeFloch, and B. Benu, "Structure and Mechanical Properties of Alkali-Alkaline Earth-Silicate Glasses," *Phys. Chem. Glasses*, **45** [1] 37–44 (2004).
- <sup>75</sup>N. Soga, "Elastic Moduli and Fracture Toughness of Glass," *J. Non-Cryst. Sol.*, **73**, 305–13 (1985).
- <sup>76</sup>V. Askapour, M. H. Manghni, and P. Richet, "Elastic Properties of Diopside, Anorthite, and Grossular Glasses and Liquids: A Brillouin Scattering Study up to 1400 K," *J. Geophys. Res.*, **98** [B10] 17683–9 (1993).
- <sup>77</sup>V. Ya Livshits, D. G. Tension, S. B. Gukasyan, and A. K. Kostanyan, "Acoustic and Elastic Properties of Glasses in the Na<sub>2</sub>O-Al<sub>2</sub>O<sub>3</sub>-SiO<sub>2</sub> System," *Sov. J. Glass Phys. Chem.*, **8**, 463–8 (1982).
- <sup>78</sup>T. Rouxel and P. Verdier, "SiC Particle Reinforced Oxynitride Glass and Glass-Ceramic Composites: Crystallization and Viscoplastic Forming Ranges," *Acta Metal Mater.*, **44** [6] 2217–25 (1996).
- <sup>79</sup>W. H. Wang, C. Dong, and C. H. Shek, "Bulk Metallic Glasses," *Mater. Sci. Eng.*, **R44**, 45–89 (2004).
- <sup>80</sup>A. Winkelmann and O. Schott, "Ueber die elasticität und über die Zug- und Druckfestigkeit verschiedener neuer gläser in ihrer abhängigkeit von der chemischen zusammensetzung," *Ann. Phys. (Leipzig)*, **51**, 697–729 (1894).
- <sup>81</sup>K. L. Loewenstein, "Studies in the Composition and Structure of Glasses Possessing High Young's Moduli. Part 1: The Composition of High Young's Modulus Glasses and the Function of Individual Ions in the Glass Structure," *Phys. Chem. Glasses*, **2** [3] 69–82 (1961).
- <sup>82</sup>W. Capps, D. H. Blackburn, A. A. Edwards, and M. Black. Nat. Bur. Stand. Repts., 3978, 4176, 4318, 4417, 4699, 4850 et 5188, 1955–1957.
- <sup>83</sup>C. J. Phillips, "Calculation of Young's Modulus of Elasticity from Composition of Simple and Complex Silicate Glasses," *Glass Technol.*, **5** [6] 216–23 (1964).
- <sup>84</sup>M. L. Williams and G. E. Scott, "Young's Modulus of Alkali-Free Glass," *Glass Technol.*, **11** [3] 76–9 (1970).
- <sup>85</sup>A. Makishima and J. D. Mackenzie, "Calculation of Bulk Modulus, Shear Modulus and Poisson's Ratio of Glass," *J. Non-Cryst. Sol.*, **17**, 147–57 (1975).
- <sup>86</sup>N. Soga, H. Yamanaka, C. Hisamoto, and M. Kunugi, "Elastic Properties and Structure of Alkaline-Earth Silicate Glasses," *J. Non-Cryst. Sol.*, **22**, 67–76 (1976).
- <sup>87</sup>L. G. Hwa, C. L. Lu, and L. C. Liu, "Elastic Moduli of Calcium Alumino-Silicate Glasses Studied by Brillouin Scattering," *Mater. Res. Bull.*, **35**, 1285–92 (2000).
- <sup>88</sup>F. J. Balta Calleja, D. S. Sanditov, and V. P. Privalko, "Review: The Microhardness of Non-Crystalline Materials," *J. Mater. Sci.*, **37**, 4507–16 (2002).
- <sup>89</sup>S. Singh, A. P. Singh, and S. S. Bhatti, "Elastic Moduli of Some Mixed Alkali Borate Glasses," *J. Mater. Sci.*, **24**, 1539–42 (1989).
- <sup>90</sup>P. Hudon and D. R. Baker, "The Nature of Phase Separation in Binary Oxide Melts and Glasses. III. Borate and Germanate Systems," *J. Non-Cryst. Sol.*, **303**, 354–71 (2002).
- <sup>91</sup>A. Khanna, K. J. S. Sawhney, M. K. Tiwari, S. Bhardwaj, and A. M. Awasthi, "Effects of Melt Ageing on the Density, Elastic Modulus and Glass Transition Temperature of Bismuth Borate Glasses," *J. Phys.: Condens. Matter*, **15**, 6659–70 (2003).
- <sup>92</sup>J. F. Ducloux and J. J. Videau, "Effect of Additional Calcium Hydroxyapatite on Sodium Borophosphate Glasses: Physical and Chemical Characterization," *Mater. Lett.*, **18**, 69–72 (1993).
- <sup>93</sup>L. L. Hench, and J. Wilson (eds.) *An Introduction to Bioceramics*. World Scientific Publishing, Singapore, 1993.
- <sup>94</sup>M. R. Reidmeyer and D. E. Day, "Phosphorous Oxynitride Glasses," *J. Non-Cryst. Sol.*, **181**, 201–14 (1995).
- <sup>95</sup>R. El Mallawany and A. Abd El Moneim, "Comparison between the Elastic Moduli of Tellurite and Phosphate Glasses," *Phys. Stat. Sol. (a)*, **166**, 829–34 (1998).
- <sup>96</sup>A. Le Sautez and R. Marchand, "Chemically Durable Nitrided Phosphate Glasses Resulting from Nitrogen/Oxygen Substitution within PO<sub>4</sub> Tetrahedra," *J. Non-Cryst. Sol.*, **263–264**, 285–92 (2000).
- <sup>97</sup>R. K. Brow, "Review: The Structure of Simple Phosphate Glasses," *J. Non-Cryst. Sol.*, **263–264**, 1–28 (2000).
- <sup>98</sup>A. H. Khafagy, "Infrared and Ultrasonic Investigations of Some [(MnO<sub>2</sub>)<sub>x</sub>(P<sub>2</sub>O<sub>5</sub>)<sub>100-x</sub>] wt% Nd<sub>2</sub>O<sub>3</sub> Glasses," *Phys. Stat. Sol. (a)*, **186** [1] 105–14 (2001).
- <sup>99</sup>T. Y. Wei, Y. Hu, and L. G. Hwa, "Structure and Elastic Properties of Low-Temperature Sealing Phosphate Glasses," *J. Non-Cryst. Sol.*, **288**, 140–7 (2001).
- <sup>100</sup>U. Hoppe, R. Kranold, H. J. Weber, and A. C. Hannon, "The Change of the Ge-O Coordination Number in Potassium Germanate Glasses Probed by Neutron Diffraction with High Real-Space Resolution," *J. Non-Cryst. Sol.*, **248** [1] 1–10 (1999).
- <sup>101</sup>Y. D. Yiannopoulos, C. P. E. Varsamis, and E. I. Kamitsos, "Density of Alkali Germanate Glasses Related to Structure," *J. Non-Cryst. Sol.*, **293–295**, 244–9 (2001).
- <sup>102</sup>A. Anan'ev, G. Karapetyan, A. Lipovskii, L. Maksimov, V. Polukhin, D. Tagantsev, B. Tatarintsev, A. Vetrov, and O. Yanush, "Multicomponent Glasses for Electroplastic Fibers," *J. Non-Cryst. Solids*, **351**, 1046–53 (2005).
- <sup>103</sup>F. R. Schilling, M. Hauser, S. V. Sinogeikin, and J. D. Bass, "Compositional Dependence of Elastic Properties and Density of Glasses in the System Anorthite-Diopside-Forsterite," *Contrib. Mineral. Petrol.*, **141**, 297–306 (2001).
- <sup>104</sup>J. Hessinger, B. E. White, and R. O. Pohl, "Elastic Properties of Amorphous and Crystalline Ice Films," *Planet. Space Sci.*, **44** [9] 937–44 (1996).
- <sup>105</sup>Y. Yue and C. A. Angell, "Clarifying the Glass-Transition Behaviour of Water by Comparison with Hyperquenched Inorganic Glasses," *Lett. Nat.*, **427**, 717–20 (2004).
- <sup>106</sup>E. L. Gromniskaya, O. V. Stal'gorova, V. V. Brazhkin, and A. G. Lyapin, "Ultrasonic Study of the Nonequilibrium Pressure-Temperature Diagram of H<sub>2</sub>O Ice," *Phys. Rev. B*, **64**, 094205 (2001).
- <sup>107</sup>[http://en.wikipedia.org/wiki/Amorphous\\_ice](http://en.wikipedia.org/wiki/Amorphous_ice). See also: [lsbu.ac.uk/water/index.html](http://lsbu.ac.uk/water/index.html).
- <sup>108</sup>M. M. Koza, B. Geil, H. Schober, and F. Natali, "Absence of Molecular Mobility on Nano-Second Time Scales in Amorphous Ice Phases," *Phys. Chem. Chem. Phys.*, **7**, 1423–31 (2005).
- <sup>109</sup>K. H. Sun, "Fundamental Condition of Glass Formation," *J. Am. Ceram. Soc.*, **30**, 277–81 (1947).
- <sup>110</sup>See for instance: Saint-Gobain Vertrotex Technical Information; [www.saint-gobainvertrotex.com](http://www.saint-gobainvertrotex.com). See also: A. S. Brown, "Spreading Spectrum of Reinforcing Fibers," *Aerospace America*, p. 14–18, January 1989.
- <sup>111</sup>R. Vacher and L. Boyer, "Brillouin Scattering: A Tool for the Measurement of Elastic and Photoelastic Constants," *Phys. Rev. B*, **6**, 639–73 (1972).
- <sup>112</sup>C. Ecolivet, "Brillouin Scattering"; pp. 129–36 in *Encyclopedia of Supramolecular Chemistry*, Edited by J. Atwood and J. Steed, M. Dekker Inc, New York, 2004.
- <sup>113</sup>A. C. Wright, "Diffraction Studies of Glass Structure: The First 70 Years," *Glass Phys. Chem.*, **24** [3] 148–79 (1998).
- <sup>114</sup>L. Cormier, L. Gалоisy, J. M. Delaye, D. Ghaleb, and G. Calas, "Short- and Medium-Range Structural Order Around Cations in Glasses: A Multidisciplinary Approach," *C.R. Acad. Sci. Paris*, **t.2** [série IV] 249–62 (2001).
- <sup>115</sup>P. H. Gaskell, "Medium-Range Structure in Glasses and Low-Q Structure in Neutron and X-Ray Scattering Data," *J. Non-Cryst. Sol.*, **351**, 1003–13 (2005).
- <sup>116</sup>J. F. Poggemann, A. Goss, G. Heide, E. Rädlein, and G. H. Frischat, "Direct View of the Structure of a Silica Glass Fracture Surface," *J. Non-Cryst. Sol.*, **281**, 221–6 (2001).
- <sup>117</sup>D. B. Miracle, "A Structural Model for Metallic Glasses," *Nat. Mater.*, **3**, 697–701 (2004).
- <sup>118</sup>H. W. Sheng, W. K. Luo, F. M. Alamgir, J. M. Bai, and E. Ma, "Atomic Packing Density and Short-to-Medium Range Order in Metallic Glasses," *Nature*, **439**, 419–25 (2006).
- <sup>119</sup>A. Lőrinczi and F. Sava, "Cluster Model of As<sub>2</sub>S<sub>3</sub> Glass," *Chalcogenide Lett.*, **2** [1] 1–3 (2005).
- <sup>120</sup>G. D. Soraru, G. D'Andrea, and A. Glisenti, "XPS Characterization of Gel-Derived Silicon Oxycarbide Glasses," *Mater. Lett.*, **27**, 1–5 (1996).
- <sup>121</sup>G. N. Greaves, "EXAFS and the Structure of Glass," *J. Non-Cryst. Sol.*, **71**, 203–17 (1985).
- <sup>122</sup>A. P. Sokolov, A. Kisliuk, M. Soltwisch, and D. Quitman, "Medium-Range Order in Glasses: Comparison of Raman and Diffraction Measurements," *Phys. Rev. Lett.*, **69** [10] 1540–3 (1992).
- <sup>123</sup>E. Duval, A. Boukenter, and T. Achibat, "Vibrational Dynamics and the Structure of Glasses," *J. Phys. Condens. Matter*, **2**, 10227–34 (1990).
- <sup>124</sup>E. Courtens, M. Foret, B. Hehlen, and R. Vacher, "The Vibrational Modes of Glasses," *Solid State Comm.*, **117**, 187–200 (2001).

- <sup>125</sup>F. P. Bos, F. A. Veer, G. J. Hobbelman, T. Romein, R. Nijse, J. Belis, P. C. Louter, and E. J. van Nieuwenhuijzen, "Designing and Planning the World's Biggest Experimental Glass Structure", pp. 401–5 in *Glass Processing Days Proceed*, Edited by J. Vitkala, Tampere, Finland, 2005. See also: www.glass.bk.tudelft.nl.
- <sup>126</sup>H. Carré and L. Daudeville, "Load-Bearing Capacity of Tempered Structural Glass," *J. Eng. Mech.*, **125** [8] 914–21 (1999).
- <sup>127</sup>J. Lindner and T. Holberndt, "Zum Nachweis von stabilitätsgefährdeten glasträgern unter biegebeanspruchung," *Stahlbau*, **75** [6] 488–98 (2006).
- <sup>128</sup>D. R. Lide (ed.) *Handbook of Chemistry and Physics*, 86th edition, Taylor & Francis, New York, 2005–2006.
- <sup>129</sup>R. D. Shannon, "Revised Effective Ionic Radii and Systematic Studies of Interatomic Distances in Halides and Chalcogenides," *Acta Cryst.*, **A32** [5] 751–67 (1976).
- <sup>130</sup>E. J. Whittaker and R. Muntus, "Ionic Radii for use in Geochemistry," *Geochim. Cosmochim. Acta*, **34**, 945–56 (1970).
- <sup>131</sup>T. M. Truskett, S. Torquato, and P. G. Debenedetti, "Towards a Quantification of Disorder in Materials: Distinguishing Equilibrium and Glassy Sphere Packings," *Phys. Rev. E*, **62** [1] 993–1001 (2000).
- <sup>132</sup>T. Aste, M. Saadatfar, A. Sakellariou, and T. J. Senden, "Investigating the Geometrical Structure of Disordered Sphere Packings," *Physica A*, **339**, 16–23 (2004).
- <sup>133</sup>"Grüneisen 1<sup>st</sup> Rule"; p. 90 in *Physical Properties of Solid Materials*, Edited by C. Zwikker, Wiley Interscience, New York, 1954.
- <sup>134</sup>E. V. Shkol'nikov, "Connection between the Microhardness and Softening Temperature and the Average Atomisation Enthalpy of Chalcogenide Glasses," *Sov. J. Glass Phys. Chem.*, **11**, 40–4 (1985).
- <sup>135</sup>P. A. G. O'Hare, A. Zywockinski, and L. A. Curtiss, "Thermodynamics of Germanium+Selenium: A Review and Critical Assessment," *J. Chem. Thermodynam.*, **28**, 459–80 (1996).
- <sup>136</sup>P. McMillan and B. Piriou, "The Structures and Vibrational Spectra of Crystals and Glasses in the Silica–Alumina Systems," *J. Non-Cryst. Sol.*, **53**, 279–98 (1982).
- <sup>137</sup>P. McMillan and B. Piriou, "Raman Spectroscopic Studies of Silicate and Related Glass Structure—A Review," *Bull. Minéral.*, **106**, 57–75 (1983).
- <sup>138</sup>S. H. Risbud, R. J. Kirkpatrick, A. P. Tagliavore, and B. Montez, "Solid-State NMR Evidence of 4-, 5-, and 6-Fold Aluminum Sites in Roller-Quenched SiO<sub>2</sub>-Al<sub>2</sub>O<sub>3</sub> Glasses," *J. Am. Ceram. Soc.*, **70**, C10–2 (1987).
- <sup>139</sup>D. R. Neuville, L. Cormier, A. M. Flank, V. Briois, and D. Massiot, "Al Speciation and Ca Environment in Calcium Aluminosilicate Glasses and Crystals by Al and Ca K-Edge X-Ray Absorption Spectroscopy," *Chem. Geol.*, **213**, 153–63 (2004).
- <sup>140</sup>S. Giri, C. Gaebler, J. Helmus, M. Affatigato, S. Feller, and M. Kodama, "A General Study of Packing in Oxide Glass Systems Containing Alkali," *J. Non-Cryst. Sol.*, **347**, 87–92 (2004).
- <sup>141</sup>H. X. Zhu, J. F. Knott, and N. J. Mills, "Analysis of the Elastic Properties of Open-Cell Foams with Tetraikaidecahedral Cells," *J. Mech. Phys. Solids*, **45** [3] 319–43 (1997).
- <sup>142</sup>R. S. Lakes, "No Contractile Obligations," *Nature*, **358**, 713–4 (1992).
- <sup>143</sup>S. D. Poisson, *Traité de Mécanique, I, II*, Courcier Pub., Paris, 1811. See also ibid: *J. Ecol. Polytechn.*, Cahier no 15 266 (1809).
- <sup>144</sup>B. Bridge and A. A. Higazy, "A Model of the Compositional Dependence of the Elastic Moduli of Multicomponent Oxide Glasses," *Phys. Chem. Glasses*, **27** [1] 1–14 (1986).
- <sup>145</sup>T. Rouxel, "The Elastic Properties of Glasses: A Multiscale Approach," 743–53, Le point sur/Review, Short Survey, CRAS Mécanique, 2B 334 (2006).
- <sup>146</sup>X. Zue and H. Toratani, "Disc Substrates for Information Recording Discs and Magnetic Discs, United States Patent 6214429 (2001). See also: www.freepatentsonline.com/6214429.
- <sup>147</sup>D. A. McGraw, "A Method for Determining Young's Modulus of Glass at Elevated Temperatures," *J. Am. Ceram. Soc.*, **35** [1] 22–7 (1952).
- <sup>148</sup>A. Winkelmann, "Ueber die elasticitätscoefficienten verschieden zusammengesetzter gläser in ihrer abhängigkeit von der temperatur," *Ann. Phys. Leipzig*, **61**, 105–41 (1897).
- <sup>149</sup>A. E. Badger and W. B. Silverman, "Modulus of Elasticity of Glass in Relation to Temperature," *J. Am. Ceram. Soc.*, **18** [9] 276–80 (1935).
- <sup>150</sup>J. M. Ide, "The Velocity of Sound in Rocks and Glasses as a Function of Temperature," *J. Geol.*, **7**, 689–716 (1937).
- <sup>151</sup>G. E. Stong, "The Modulus of Elasticity of Glass: I. Preliminary Studies: (a) Effect of Thermal History; (b) Effect of Temperature Change," *J. Am. Ceram. Soc.*, **20** [1] 16–22 (1937).
- <sup>152</sup>K. Franke, "Der elasticitätsmodul einiger technischer gläser in abhängigkeit von der temperatur," *Glastech. Berichte*, **4**, 113–9 (1941).
- <sup>153</sup>J. Gillod, "Le module d'élasticité et l'état structural des verres," *Verres Réfract.*, **1**, 26–33 (1946).
- <sup>154</sup>S. Spinner, "Elastic Moduli of Glasses at Elevated Temperatures by a Dynamic Method," *J. Am. Ceram. Soc.*, [3] 113–8 (1956).
- <sup>155</sup>G. J. Dienes, "The Temperature Dependence of the Elastic Moduli of Vitreous Silica," *J. Phys. Chem. Sol.*, **7**, 290–4 (1958).
- <sup>156</sup>M. J. Kerper and T. G. Scuderi, "Mechanical Properties of Glass at Elevated Temperature," *Ceram. Bull.*, **42** [12] 735–40 (1963).
- <sup>157</sup>H. Bornhöft and R. Brückner, "Ultrasonic Measurements and Complex Elastic Moduli of Silicate Glass Melts in the Viscoelastic and Viscous Range," *Glastech. Ber. Glass Sci. Technol.*, **67** [9] 241–54 (1994).
- <sup>158</sup>E. P. Papadakis, K. A. Fowler, L. C. Lynnworth, A. Robertson, and E. D. Zysk, "Ultrasonic Measurements of Young's Modulus and Extensional Wave Attenuation in Refractory Metal Wires at Elevated Temperatures with Application to Ultrasonic Thermometry," *J. Appl. Phys.*, **45** [6] 2409–20 (1974).
- <sup>159</sup>C. Gault, "Ultrasonic Non-Destructive Evaluation of Microstructural Changes in Degradation of Ceramics at High Temperature," *Mater. Res. Soc. Symp. Proc.*, **142**, 263–75 (1989).
- <sup>160</sup>Y. Y. Huang, J. L. Hunt, and J. R. Stevens, "Determination of Elastic Constants in Isotropic Silicate Glasses by Brillouin Scattering," *J. Appl. Phys.*, **44** [8] 3589–92 (1973).
- <sup>161</sup>J. Kieffer, "Mechanical Degradation and Viscous Dissipation in B<sub>2</sub>O<sub>3</sub>," *Phys. Rev. B*, **50** [1] 17–31 (1994).
- <sup>162</sup>L. Donzel, A. Lakki, and R. Schaller, "Glass Transition Temperature and a Relaxation in Y–Si–Al–O–N Glasses and in Si<sub>3</sub>N<sub>4</sub> Ceramics Studied by Mechanical Spectroscopy," *Philos. Mag. A*, **76** [5] 933–44 (1997).
- <sup>163</sup>G. Roebben, B. Bollen, A. Brebels, J. Van Humbeeck, and O. Van der Biest, "Impulse Excitation Apparatus to Measure Resonant Frequencies, Elastic Moduli, and Internal Friction at Room and High Temperature," *Rev. Sci. Instr.*, **68** [12] 4511–5 (1997).
- <sup>164</sup>P. Gadaud and S. Pautrot, "Characterization of the Elasticity and Anelasticity of Bulk Glasses by Dynamical Subresonant and Resonant Techniques," *J. Non-Cryst. Sol.*, **316**, 146–52 (2003).
- <sup>165</sup>E. Le Bourhis, P. Gadaud, J-P. Guin, N. Tournerie, X-H. Zhang, J. Lucas, and T. Rouxel, "Temperature Dependence of the Mechanical Behaviour of a Ge-As-Se Glass," *Script. Mater.*, **45**, 317–23 (2001).
- <sup>166</sup>C. A. Angell, "Perspective on the Glass Transition," *J. Phys. Chem. Sol.*, **49** [8] 863–71 (1988).
- <sup>167</sup>T. Rouxel, J. C. Sangleboeuf, M. Huger, C. Gault, J-L. Besson, and S. Testu, "Temperature Dependence of Young's Modulus in Si<sub>3</sub>N<sub>4</sub>-Based Ceramics: Role of Sintering Additives and of SiC-Particle Content," *Acta Mater.*, **50**, 1669–82 (2002).
- <sup>168</sup>A. Polian, D. Vo-Thanh, and P. Richet, "Elastic Properties of a-SiO<sub>2</sub> up to 2300 K from Brillouin Scattering Measurements," *Europhys. Lett.*, **57** [3] 375–81 (2002).
- <sup>169</sup>J. A. Bucaro and H. D. Dardy, "High-Temperature Brillouin Scattering in Fused Quartz," *J. Appl. Phys.*, **45** [12] 5324–9 (1974).
- <sup>170</sup>M. L. Vaillant, V. Keryvin, T. Rouxel, and Y. Kawamura, "Changes in the Mechanical Properties of a Zr<sub>55</sub>Cu<sub>30</sub>Al<sub>10</sub>Ni<sub>5</sub> Bulk Metallic Glass Due to Heat-Treatments below 540°C," *Script. Mater.*, **47**, 19–23 (2002).
- <sup>171</sup>T. Ichitubo, E. Matsubara, H. S. Chen, J. Saida, T. Yamamoto, and N. Nishiyama, "Structural Instability of Metallic Glasses Under Radio-Frequency-Ultrasonic Perturbation and its Correlation with Glass-to-Crystal Transition of Less-Stable Metallic Glasses," *J. Chem. Phys.*, **125**, 154502 (2006).
- <sup>172</sup>W. M. Slie, A. R. Donfor, and T. A. Litovitz, "Ultrasonic Shear and Longitudinal Measurements in Aqueous Glycerol," *J. Chem. Phys.*, **44** [10] 3712–8 (1966).
- <sup>173</sup>R. Kono, "The Dynamic Bulk Viscosity of Polystyrene and Polymethyl Methacrylate," *J. Phys. Soc. Jpn.*, **15** [4] 718–25 (1960).
- <sup>174</sup>R. E. Youngman, J. Kieffer, J. D. Bass, and L. Duffrène, "Extended Structural Integrity in Network Glasses and Liquids," *J. Non-Cryst. Sol.*, **222**, 190–8 (1997).
- <sup>175</sup>A. K. Hassan, L. M. Torell, L. Börjesson, and H. Doweidar, "Structural Changes of B<sub>2</sub>O<sub>3</sub> through the Liquid–Glass Transition Range: A Raman-Scattering Study," *Phys. Rev. B*, **45** [22] 12797 (1992).
- <sup>176</sup>L. Huang and J. Kieffer, "Amorphous–Amorphous Transitions in Silica Glass. I. Reversible Transitions and Thermomechanical Anomalies," *Phys. Rev. B*, **69**, 224203 (2004).
- <sup>177</sup>D. J. Lacks, "First-Order Amorphous–Amorphous Transformation in Silica," *Phys. Rev. Lett.*, **84** [20] 4629–32 (2000).
- <sup>178</sup>J. E. Masnik, J. Kieffer, and J. D. Bass, "The Complex Mechanical Modulus as a Structural Probe—The Case of Alkali Borate Liquids and Glasses," *J. Chem. Phys.*, **103** [23] 9907–17 (1995).
- <sup>179</sup>R. Böhmer, K. L. Ngai, C. A. Angell, and D. J. Plazek, "Nonexponential Relaxations in Strong and Fragile Glass Formers," *J. Chem. Phys.*, **99** [5] 4201–9 (1993).
- <sup>180</sup>S. A. Brawer, "Theory of Relaxation in Viscous Liquids and Glasses," *J. Chem. Phys.*, **81** [2] 954–74 (1984).
- <sup>181</sup>V. N. Novikov and A. P. Sokolov, "Poisson's Ratio and the Fragility of Glass Forming Liquids," *Lett. Nat.*, **431**, 961–3 (2004).
- <sup>182</sup>S. N. Yannopoulos and G. P. Johari, "Poisson's Ratio and Liquids Fragility," *Nature*, **442**, E7–E8 (2006).
- <sup>183</sup>A. Concell, G. Alcalá, S. Mato, T. G. Woodcock, A. Gebert, J. Eckert, and M. D. Baro, "Effect of Relaxation and Primary Nanocrystallization on the Mechanical Properties of Cu<sub>60</sub>Zr<sub>22</sub>Ti<sub>18</sub> Bulk Metallic Glass," *Intermetallics*, **13**, 1214–9 (2005).
- <sup>184</sup>C. R. Kurkjian, J. T. Krause, H. J. McSkimmin, P. Andreatch, and T. B. Bateman, "Pressure Dependence of Elastic Constants and Grüneisen Parameters in Fused SiO<sub>2</sub>, GeO<sub>2</sub>, BeF<sub>2</sub> and B<sub>2</sub>O<sub>3</sub>," p. 45 in *Amorphous Materials*, Edited by R. W. Douglas and B. Ellis, Wiley-Interscience, London, 1970.
- <sup>185</sup>S. C. Zha, R. J. Hemley, H. K. Mao, T. S. Duffy, and C. Meade, "Acoustic Velocities and Refractive Index of SiO<sub>2</sub> Glass to 57.5 GPa by Brillouin Scattering," *Phys. Rev. B*, **50** [18] 13105–12 (1994).
- <sup>186</sup>K. Kondo, S. Ito, and A. Sawaoka, "Nonlinear Pressure Dependence of the Elastic Moduli of Fused Quartz up to 3 GPa," *J. Appl. Phys.*, **52** [4] 2826–31 (1981).
- <sup>187</sup>S. Yoshida, J. C. Sangleboeuf, and T. Rouxel, "Quantitative Evaluation of Indentation-Induced Densification in Glass," *J. Mater. Res.*, **20**, 3404–12 (2005).
- <sup>188</sup>T. Rouxel and F. Wakai, "The Brittle to Ductile Transition in a Si<sub>3</sub>N<sub>4</sub>/SiC Composite with a Glassy Grain Boundary Phase," *Acta Met. Mater.*, **41** [11] 3203–13 (1993).
- <sup>189</sup>K. Tanaka, T. Ichitubo, and E. Matsubara, "Elasticity and Anelasticity of Metallic Glass Near the Glass Transition Temperature," *Mater. Sci. Eng., A*, **442**, 278–82 (2006).
- <sup>190</sup>C. C. Chen, Y. J. Wu, and L. G. Hwa, "Temperature Dependence of Elastic Properties of ZBLAN Glasses," *Mater. Chem. Phys.*, **65**, 306–9 (2000).
- <sup>191</sup>H. Hensenkemper and R. Brückner, "Elastic Constants of Glass Melts above the Glass Transition Temperature from Ultrasonic and Axial Compression Measurements," *Glastechnol. Ber.*, **64** [2] 29–38 (1991).

<sup>192</sup>V. Keryvin, M. L. Vaillant, T. Rouxel, M. Huger, T. Gloriant, and Y. Kawamura, "Thermal Stability of a  $Zr_{55}Cu_{30}Al_{10}Ni_5$  Bulk Metallic Glass Studied by *In Situ* Ultrasonic Echography," *Intermetallics*, **10**, 1289–96 (2002).

<sup>193</sup>T. Rouxel et al and J. C. Sangleboeuf, "The Brittle to Ductile Transition in a Soda–Lime–Silica Glass," *J. Non-Cryst. Sol.*, **271**, 224–35 (2000).

<sup>194</sup>K. Schröter and E. Donth, "Comparison of Shear Response with Other Properties at the Dynamic Glass Transition of Different Glassformers," *J. Non-Cryst. Sol.*, **307–310**, 270–80 (2002).

<sup>195</sup>R. Böhmer and C. A. Angell, "Correlations of the Nonexponentiality and State Dependence of the Mechanical Relaxations with Bond Connectivity in Ge–As–Se Supercooled Liquids," *Phys. Rev. B*, **45** [17] 10091–4 (1992).

<sup>196</sup>Results Extracted from Mechanical Relaxation Experiments Performed by the Author in Compression in the 1173–273 K Temperature Range. Unpublished data.

<sup>197</sup>T. Rouxel, B. Baron, P. Verdier, and T. Sakuma, "SiC Particle Reinforced Oxynitride Glass: Stress Relaxation, Creep and Strain-Rate Imposed Experiments," *Acta Mater.*, **46**, 6115–30 (1998).

<sup>198</sup>M. Blétry, P. Guyot, J. J. Blandin, and J. L. Soubeyroux, "Free Volume Model: High-Temperature Deformation of a Zr-Based Bulk Metallic Glass," *Acta Mater.*, **54**, 1257–63 (2006).

<sup>199</sup>M. Huger and T. Chotard, ENSCI (Limoges), Internal Report (2005).

<sup>200</sup>S. Maillard, "Fissuration et autoréparation des liants bitumineux"; Ph.D. Report, LCPC-ECN, Nantes, France (2005). □



Tanguy Rouxel obtained his B. Sc (French DEA) in Mechanics of Materials from the University of Paris XIII, and his Ph.D. (French Doctorate) in Ceramic Science from the University of Limoges. After graduating he became a Post-doctoral Fellow in the Government Industrial Research Institute of Nagoya (then the NIRIN, Japan) for one and a half years. Dr. Rouxel then held a position as a CNRS Researcher in the Ecole Nationale Supérieure de Céramiques Industrielles. In 1997, Dr. Rouxel was appointed Professor at the University of Rennes, where the FFAG (Flow and Fracture in Advanced Glasses) meetings started in 2001. FFAG4 is being planned for Shiga (Japan) in November 2007. Dr. Rouxel received the Academic Prize from the Ceramic Society of France (GFC) in 1992, the brass medal from CNRS (1996), the AYCECT (Asia Young Ceramist Conference in Tokai) Prize (2006), and the Yvan Peyches Awards from the French Academy of Sciences (2007).